Resistance Committee

Final Report and Recommendations to the 27th ITTC

1. INTRODUCTION

1.1 Membership and Meetings

The members of the Resistance Committee of the 27th ITTC are:

- Prof. Stephen Turnock (Chair) University of Southampton
  Southampton, United Kingdom
- Dr. Hisao Tanaka
  Japan Marine United Corporation
  Tsu, Japan
- Dr. Jin Kim
  Maritime and Ocean Engineering Research Institute
  Daejeon, Korea
- Prof. Baoshan Wu
  China Ship Scientific Research Centre
  Wuxi. Jiangsu, China
- Dr. Thomas C. Fu (Secretary)
  Naval Surface Warfare Center, Carderock Division
  W. Bethesda, Maryland, U.S.A.
- Prof. Ali Can Takinaci
  Istanbul Technical University
  Istanbul, Turkey
- Dr. Tommi Mikkola
  Aalto University
  Helsinki, Finland

Four committee meetings have been held during the work period:

- Istanbul, Turkey, 27-28 February 2012 at the Istanbul Technical University.
- Bethesda, Maryland, U.S.A., 13-14 September 2012 at the Naval Surface Warfare Center Carderock Division.
- Espoo, Finland, 10-11 June 2013 at Aalto University, Otaniemi Campus.
- Southampton, United Kingdom, 14-15 January 2014 at the University of Southampton.

1.2 Tasks

The recommendations for the work of the Resistance Committee as given by the 26th ITTC were as follows:

1. Update the state-of-the-art for predicting the resistance of different ship concepts emphasising developments since the 2011 ITTC Conference. The committee report should include sections on:

a. The potential impact of new technological developments on the ITTC.

b. New experimental techniques and extrapolation methods.

c. New benchmark data.

d. The practical applications of computational methods to resistance predictions and scaling.

e. The need for R&D for improving methods of model experiments, numerical modeling and full-scale measurements.

2. Review ITTC Recommended Procedures relevant to resistance and:

   a. Identify any requirements for changes in the light of current practice, and, if approved by the Advisory Council, update them.

   b. Identify the need for new procedures and outline the purpose and content of these.

   c. Implement updated uncertainty analysis spreadsheet for resistance test.

3. Continue the analysis of the ITTC worldwide series for identifying facility biases.

4. Review definitions of surface roughness and develop a guideline for its measurement.

5. Review results from tests that correlate skin friction with surface roughness.

6. Review trends and new developments in experimental techniques on unsteady flows and dynamic free surface phenomena.

7. Review new developments on model manufacturing devices and methods.

8. Review the development and evaluate improvements in design methods and the capabilities of numerical optimization applications, such as Simulation Based Design environments, with special emphasis on design of new ship concepts, geometry manipulation and parameterization, surrogate models and variable fidelity applications. (The fundamental assumption that an optimal hull shape is one that minimizes the calm water resistance may no longer be appropriate given the developments in CFD that give the designer the ability to make assessment of both wave and viscous effects for added resistance in waves as well as the interaction between hull-propulsor and appendages.)

2. STATE OF THE ART

The concern of the shipping industry to both reduce fuel use and hence expense, as well emissions, has placed greater emphasis on the ability to accurately resolve at design small changes in hull and appendage resistance. This desire has driven many of the state-of-the-art improvements seen since 2011 as the results of funded research programmes focussed on the energy efficiency design index (EEDI) start to reach maturity.

A review by Molland et al (2014) compares alternative techniques for improving overall ship propulsive efficiency for both drag reduction and improved propulsor efficiency. Table 1 compares the relative contributions of different resistance components for a variety of ship types. The domination of skin friction, especially at slow speeds, confirms the research drive to improve coatings longevity and performance as well the search for alternative

methods of reducing friction such as air lubrication. One area which has received little attention to date is in methods to reduce air resistance of ship superstructures which although they constitute 2-4% of resistance are treated effectively as a bluff body dominated by pressure form drag (Molland et al, 2011). As such they are well suited to a relatively simple series of design modification. Investigations using a combination of CFD and wind tunnel tests are expected to result in a new generation of streamlined ships.

Table 1 Approximate distribution of resistance components. Air drag is shown as a percentage of total resistance, i.e. total hull plus appendages plus air.(Molland et al, 2014)

Type	Lbp (m)	C_B	Dw (tonnes)	Service speed (Knots)	Service power (kW)	*Fr*	Hull resistance component			Air Drag % total
							Friction %	Form %	Wave %	
Tanker	330	0.84	250000	15	24000	0.136	66	26	8	2.0
Tanker	174	0.80	41000	14.5	7300	0.181	65	25	10	3.0
Bulk carrier	290	0.83	170000	15	15800	0.145	66	24	10	2.5
Bulk carrier	180	0.80	45000	14	7200	0.171	65	25	10	3.0
Container	334	0.64	100000 10000 TEU	26	62000	0.234	63	12	25	4.5
Container	232	0.65	37000 3500 TEU	23.5	29000	0.250	60	10	30	4.0
Catamaran ferry	80	0.47	650 pass 150 cars	36	23500	0.700	30	10	60	4.0

One method of reducing resistance is that of adjusting the in service trim of vessels and this has prompted a significant number of towing tank studies. Larsen et al (2012) examined the physics of how adjusting trim can modify both the form and wave resistance components. They used a combination of model tests, RANS CFD, and potential flow theory to investigate the behaviour of a large cargo vessel at partially loaded draught and reduced speed. The RANS CFD was used to calculate the resistance and as shown in Figure 1 captured well the changes found in the model scale self propulsion tests, whereas the potential flow under predicted the power change. Overall a 10% drop in power could be achieved with the correct trim, with 80% originating from reduction in residuary resistance around the bulbous bow.

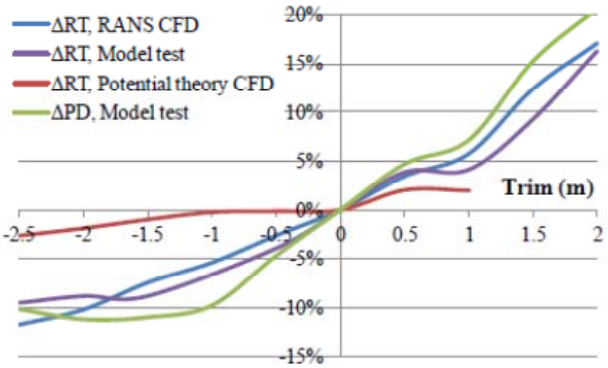

Figure 1. Comparison of different trim guidance methods at Fn=0.128 (Larsen et al, 2012).

The ability of CFD to resolve in detail the flow features around the bulbous wave which initiate the drag changes with trim is captured well in Figure 2. An example of a study for a shipping fleet (Takinaci and Onen,2013) on trim optimisation found 4-14% power reduction for a range of size of ships. Ships in the range of 40,000-80,000 tonnes had important

potential benefits, whereas for larger ships the gains were found to be less.

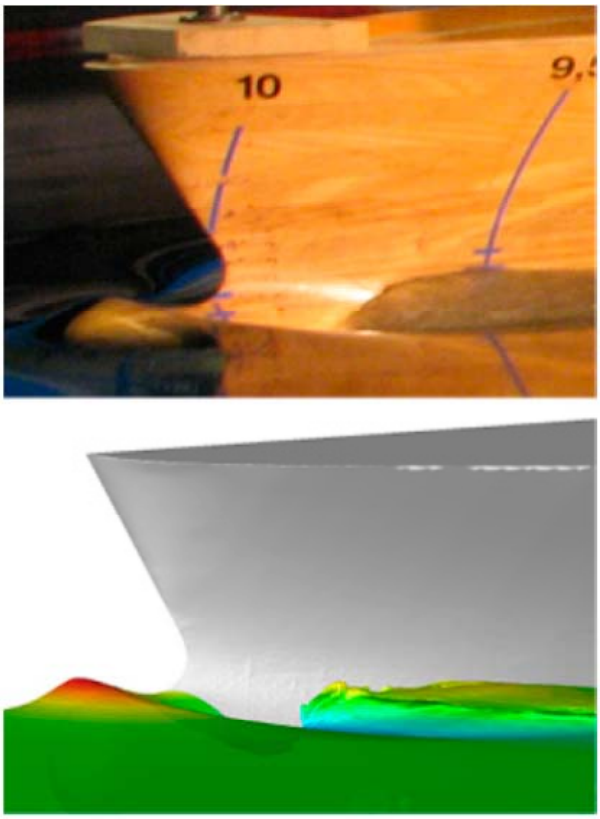

Figure 2. Bow wave at 2.0m trim and Fn=0.128.Model test and RANS CFD (Larsen et al, 2012).

Another area of growing importance is the understanding of the influence of detailed hull design on added resistance effects. In the past designing a ship for a single design speed, matching the propulsor in calm water, and then adding an appropriate powering margin was acceptable. The influence of the installed power term in the EEDI formula now challenges designers to at least consider how they can better quantify the performance of the ship across its whole operational profile. A probabilistic approach can be applied for the expected voyage sea states that allows a better assessment to be made of alternative hull designs. For example Winden et al (2013) studied, using CFD, the influence of added and calm water resistance in steady waves of a variety of bow forms, shown in Figure 3.

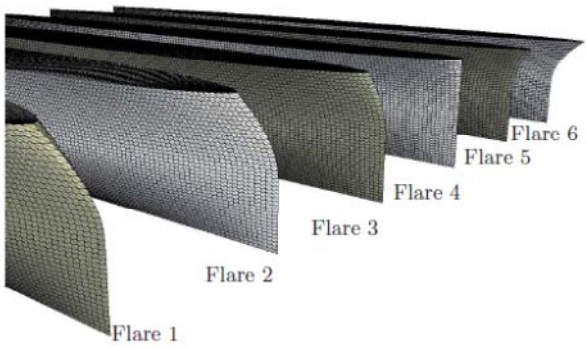

Figure 3. Six flares used to assess influence on added resistance (Winden et al, 2013).

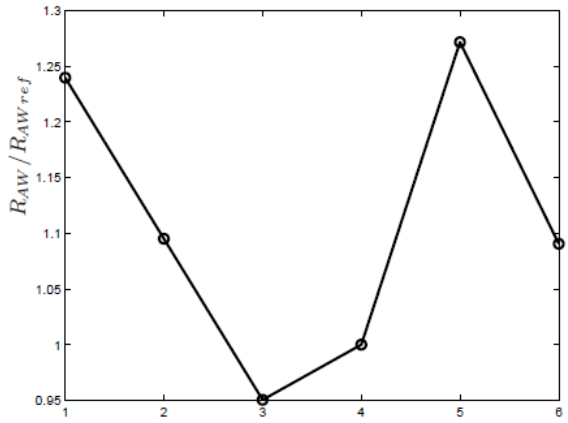

Figure 4. Added resistance in waves for the tested bow sections.

Significant changes can be found as given in Figure 4 for the change in added resistance compared to the reference hull. There is limited available experimental data for validation of computational approaches but as described later in section 8 the ever growing capability of simulation based techniques will require such data to ensure that valid designs are implemented at full scale.

2.1 New Technologies

Air lubrication. As one of the energy-saving technologies, frictional drag reduction technology by air lubrication has been developed and its practical use is being attempted, see for example Kawakita (2013).

Kawashima et al. (2007) gives a progress report of a research project moving towards practical use of air bubble injection as a drag reduction device for ships. The project aims to achieve a 10% net energy-saving by air bubble injection, taking into account the work needed for injecting air bubbles.

It is difficult to estimate the actual drag reduction effect on a full scale ship based on model scale experiments, as the relative scale ratio of air bubbles to boundary layer length is very different between model and actual ship. Therefore they carried out experiments using a flat plate (L = 50 m, B = 1 m) in the 400 m towing tank of NMRI. The plate was towed at 6.2 m/s (12 kt), which equivalent to the cruising speed of the ship for a full scale experiment. Air bubbles were injected at 3 m from the bow. Both the total drag of the flat plate and local skin friction were measured. The procedure of the power estimation of the full scale ship in the state of the bubble injection is shown in Figure 5. The skin friction drag reduction values by bubbly flow in full scale ship are estimated based on tank test result of flat plate. The drag reduction value in full scale ship with bubble flow drag reduction system is estimated based on a linear approximation. An example of estimation is shown in Figure 6.

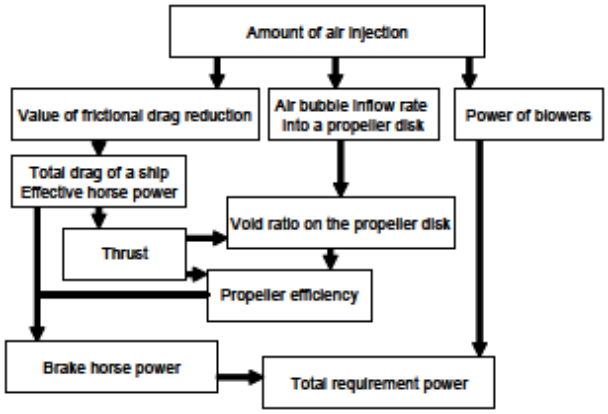

Figure 5. Schematic diagram of full scale ship power estimation with bubble flow drag reductions system.(Kawashima et al, 2007)

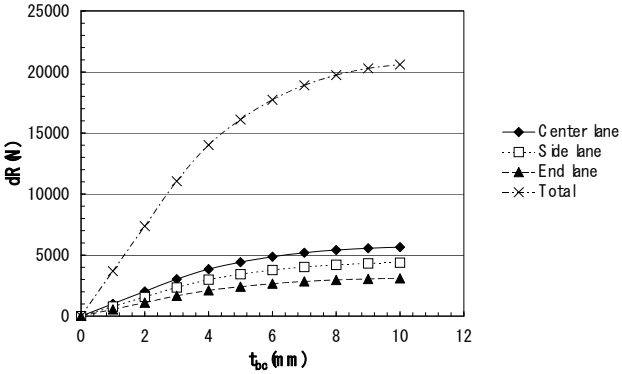

Figure 6. Estimation of drag reduction value in full scale ship with bubble flow drag reduction system based on curve approximation. (Kawashima et al, 2007)

2.2 Experimental Techniques and Extrapolation

The advanced model measurement technology conference series organised via an EU sponsored research programme, the hydro testing alliance http://www.hta-forum.eu/, provides a valuable resource of up-to-date developments in experimental testing technology. The 3rd of the series was held in Gdansk in September

2013, Atlar and Wilczynski, (2013). The sessions concentrated on noise measurements, PIV applications, optical measurements, coating assessment and drag reduction, uncertainty, control technologies, free running models and smart tank testing.

Of relevance to the later discussion of CFD validation for resistance prediction is the method of waterline registration using fluorescence, Geerts et al (2011). Waterline registration is of use in assessing squat, freeboard and bow wave dynamics. The use of a fluorescent light source applied as a coating to the hull and illuminated by UV prevents unwanted reflections and allows much more accurate capture of the dynamic surface waterline as shown in Figure 7.

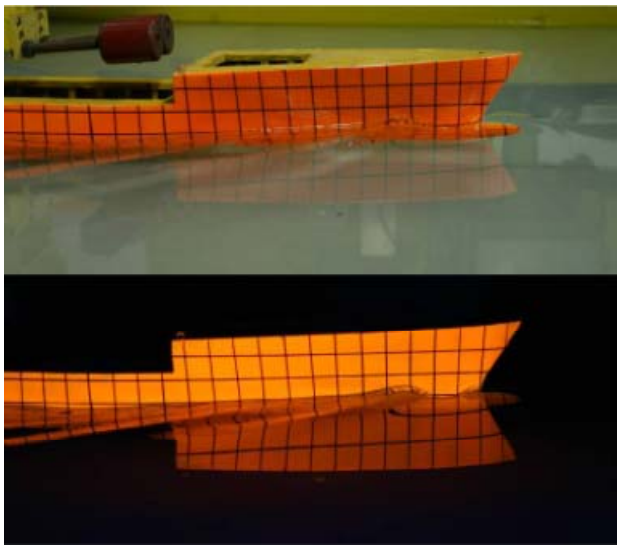

Figure 7. Comparison of an image from the same camera position but with different lighting at a model speed of 0.65 m/s; above: image with regular tank lights, below: image with ultra violet lights.

The rapid reduction in the cost of inertial measurement units and their ease of use, either through use of commercial 'smartphone' systems or as more conventional instrument packages provides an alternative method of measuring model sinkage and trim. Bennett et al (2014) used a combination of three 9 degree of freedom wireless sensors, strain gauges, conventional heave and trim potentiometers and video analysis to investigate model response. Figure 8 shows the experimental setup. An experimental uncertainty analysis demonstrated that with suitable calibration comparable levels of uncertainty were obtained between the conventional heave and pitch measurements and those obtained derived using calibrated wireless sensors. Such systems are ideal for use on free running models were conventional techniques are not applicable and often video motion capture systems are difficult to use due to lighting or location of suitable fixture locations.

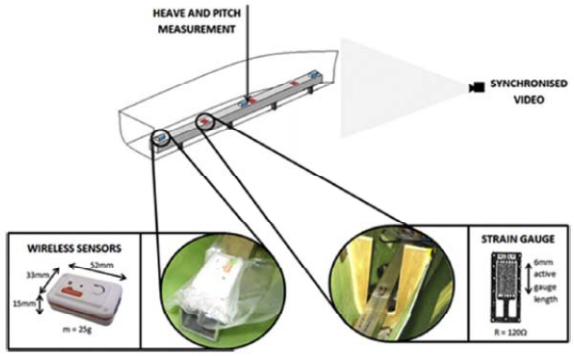

Figure 8. Schematic of experimental set-up of a segmented hydroelastic model with three Shimmer sensors.

2.3 New Benchmark Data,

The results of a major new experimental study for bench-marking data are not reported in this term of the Committee. But the plan of new measurements is confirmed with the Steering Committee for CFD Workshop 2015 (Larsson et al, 2014) and it will be used as the new benchmark case. The Workshop will be held at Tokyo in December 2-4, 2015. The detail information can be found at http://www.t2015.nmri.go.jp, the workshop

website. The model ship is named as Japan Bulk Carrier (JBC). The lines of JBC hull form are shown in Figure 9 and 10. The JBC hull form has a duct type ESD (energy saving device) and so the experimental data will be obtained both with and without a duct. The model size and measurement items are shown in Table 2.

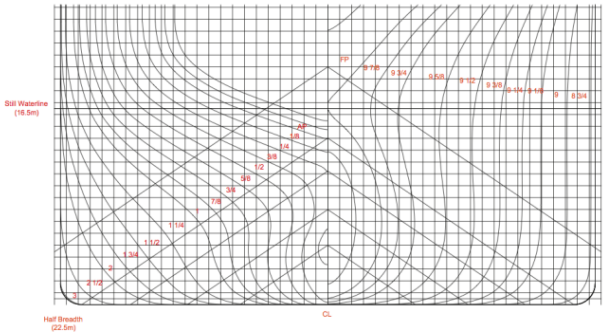

Figure 9. Body plan of JBC

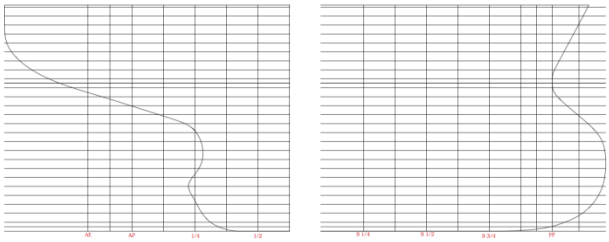

Figure 10. Profile of JBC

Table 2. Items of measurement for JBC

Condition	Hull	Measurement	Towing Tank
Towing	7m BH	X, M	NMRI
	7m BH w/o ESD	V, T	NMRI
	7m BH w/ ESD	V, T	NMRI
	3m BH w/o ESD	V, T	OU
	3m BH w/ ESD	V, T	OU
Self-prop	7m BH	SP, M	NMRI
	7m BH w/o ESD	V, T	NMRI
	7m BH w/ ESD	V, T	NMRI
	3m BH w/o ESD	V, T	OU
	3m BH w/ ESD	V, T	OU

*X: Resistance, M: Trim and Sinkage, SP: Self-propulsion data, V: Velocities, T: Turbulence, NMRI: National Maritime Research Institute, OU: Osaka University

2.4 Practical Applications of CFD

A good overview of the current capabilities of the CFD methods in ship hydrodynamics is provided by the CFD Workshop series. An interested reader is also referred to an extensive review of current capabilities and future trends of CFD in ship hydrodynamics by Stern et al (2013), which includes collected results and references on various resistance, sinkage and trim verification and validation studies. The latest Gothenburg 2010 workshop was quite extensively discussed in the report of the 26th ITTC Specialist committee on CFD. However, a book (Larsson et al, 2014) about the results, findings and conclusions of the workshop has been published recently with some additional experimental and computational data. For completeness it is appropriate to collect some of the conclusions of the workshop which are most relevant for resistance and the associated flow predictions.

- Considering all the computed resistance predictions the mean difference between measurements and simulations is practically zero (-0.1%) and the mean standard deviation has improved considerably since the 2005 workshop (from 4.7% to 2.1%). The average comparison errors in sinkage and trim for Fr>0.2 are around 4%, whereas larger (relative) errors are observed for lower speeds most probably due to difficulties in measuring the quantities accurately and due to the small absolute values. Wave profiles on the hull and at the closest cut are generally well predicted, but large differences between the methods are observed further from the hulls.

- Grid sizes above 3 million cells do not provide discernible improvement in resistance predictions (with URANS). Above and below this the resistance predictions are within 4% and 8% of the measured value. Finer grids with up to tens of millions of cells are required for local flow predictions. For DTMB 5415 accurate free-surface prediction can be obtained with just 2 million cells whereas finer grid are required for KVLCC2 due to shorter wave length.

- The results suggest that turbulence models more advanced than the two-equation models do not improve the resistance predictions. The anisotropic explicit algebraic Reynolds stress model seems to be the best option for predicting aft body flow of U shaped hulls with strong bilge vortex. The hybrid RANS/LES models seem promising, but they show limitations for flows with limited separation or triggering turbulence for slender bodies. Furthermore, the grid resolution requirements are significantly higher than for URANS based predictions.

- The results suggest that it is easier to reach convergent behaviour with grid variation using structured rather than unstructured grids. The established uncertainty estimation methods give consistent results in the vicinity of the asymptotic range, but quite different estimates far from the range. Most resistance solutions are validated. For the non-validated solutions the source of error is suggested to be the turbulence model.

The favourable characteristics of an anisotropic turbulence model have been demonstrated by Guo et al (2013) as well. They have studied the distribution of resistance by measuring and simulating the calm water resistance, sinkage and trim of a three-segment KVLCC2 model. A comprehensive verification and validation study shows that both isotropic and anisotropic models can give good prediction in terms of the measured quantities, but the superiority of the anisotropic explicit algebraic stress model is revealed by the resistance prediction of the aft segment. The study provides particularly interesting reference data for CFD model validation.

As the methods have matured and the modelling knowledge has increased, Navier-Stokes equations based methods are used for an increasingly wide range of cases related to resistance and wave making. Castiglione et al (2014) have studied the validity of the RANS based resistance prediction for a catamaran model in shallow water and the influence of water depth of the interference effects. Maki et al (2013) have compared linear potential flow and RANS based methods for the prediction of the calm-water resistance components of a surface effect ship. Takai et al (2011) have studied the predictive capability of RANS based approach for the performance analysis of a very large high-speed ship with a transit speed of at least 36 knots. Bhushan et al (2012) have studied the vortical structures and the associated transom flow and sinkage and trim instabilities of the appended Athena hull form using hybrid

RANS/LES approach including validation against full-scale experimental data.

Examples of current and future capabilities of CFD with massively parallel simulations have been provided by Nishikawa et al (2012, 2013) and Fu et al (2013). Nishikawa et al (2012) have demonstrated fully resolved LES of KVLCC2 with Reynolds numbers of $5x10^5$ and $1x10^6$ with up to $1x10^9$ cells and over 1500 cores and later (Nishikawa et al, 2013) with model test Reynolds number $4.6x10^6$ using up to $32x10^9$ cells.

These papers provide concrete examples of the rapid development of high performance computing and of the computational requirements of fully resolved LES simulations with practical Reynolds numbers. Fu et al (2013) on the other hand have studied the capabilities of a Cartesian grid immersed body, volume-of-fluid method for the simulation of planing hulls. They have compared measurements and massively parallel simulations with $1\text{-}8x10^8$ cells for three validation cases. The results demonstrate excellent reproduction of the flow details such as impact pressure, wetted length and spray sheet formation and good agreement in terms of hull attitude and resistance.

Despite the rapidly growing interest in bare hull flow and resistance predictions based on the Navier-Stokes equations with (U)RANS, LES or DES modelling, there is still an interest to apply and develop potential flow based methods also for resistance predictions (see also the section on simulation based design). The methods have been improved both in terms of predictive capability and computational efficiency. Huang et al (2013) discuss the numerical implementation of the Neumann-Michell theory of ship generated waves. They highlight the importance of specific implementation details which are fundamental for the quality of the predictions. The developed approach provides a resistance prediction with an accuracy of around 10 percent for a wide range of displacement hull forms and Froude numbers.

Belibassakis et al (2013) have applied isogeometric analysis for the Neuman-Kelvin problem of the ship wave making and resistance. Here the same NURBS basis is used to define the geometry and the singularity distributions with the intention of providing the same accuracy with a lower number of panels and a natural connection with modern ship design systems. Taravella and Vorus (2012) have developed an expanded, general solution of Ogilvie's formulation for moderate and high-speed ships ($0.4<Fr<1.0$) accounting for the wake trench generated by a fully ventilated transom. For the three cases shown with closed stern or fully ventilated transom the accuracy of the resistance prediction is roughly 10 percent from Fr=0.4 up. Yan and Liu (2011) have applied the Pre-corrected Fast Fourier Transform (PFFT) to improve the computational efficiency of the high-order boundary element method (BEM) for nonlinear wave-wave/body interaction. The approach is based on a process, where only the near-field contributions of the influence matrix are evaluated exactly. The approach reduces the $O(N^{2\sim3})$ expense of the conventional quadratic BEM to $O(N \ln N)$. Series 60 has been used as a practical case to demonstrate the applicability of the developed approach.

In terms of verification and validation of computational predictions Eca and Hoekstra (2014) have proposed a new procedure for the estimation of numerical uncertainty. They have combined the traditional variable order expansion (ah^p) and three alternative fixed order expansions (ah, ah^2, $a_1h + a_2h^2$). The procedure includes non-weighted and weighted fits and the best fit is selected based on the standard deviation of the fit. The procedure is tested with four different test cases including the re-

sistance of KVLCC2. It is demonstrated that the alternative expansions are more frequently used as the complexity of the flow case increases. The results further demonstrate that it is hard to avoid scatter of data in complex flow cases and, thus uncertainty estimation procedures which are able to handle this are required.

An extensive analysis by Zou and Larsson (2014) of all the Gothenburg 2010 compares alternative approaches for verification and validation on the large data set of mesh refinement triplets. These indicate that for the various approaches tested that verification and validation gives a relatively reliable error and uncertainty estimation when used within the asymptotic region. That the level of iterative convergence needs to be assessed alongside grid convergence and that typically modelling error is small compared to numerical and experimental uncertainty.

2.5 Need for Research and Development

As the need for increased energy efficiency has grown, the number of unconventional hull forms, drag reduction technologies, and interest in multihulls has also grown. In order to effectively assess the performance of these technologies and designs, including their performance at sea in a range of sea states much research is needed in improving instrumentation and testing methods both at model and full scales, in the numerical modelling and understanding the physics related to ship resistance. Specifically work needs to be done as it relates to high-speed planing hulls, multi-hulls, drag reduction technologies, and added resistance in waves. Advances in numerical modelling continue, but increased emphasis on improved turbulence modelling and focus on simulation of high Reynolds number boundary layers, and high Froude number flows are needed to both support advanced concept design and accurate prediction on ship flows and hydrodynamics forces. The ability to predict accurately viscous drag, wave drag, form drag (pressure) and spray drag continues to be of importance and continued work is needed. Schemes for handling surface roughness numerically still remain an area of research as is the accurate modelling of full-scale boundary layers. Wave interactions between multihull hulls continue to be a challenge, as is the accurate prediction of spray drag for high-speed craft.

With the current emphasis on energy efficiency, systems that provide weather routing to save fuel have been proposed. These systems rely on accurate prediction and knowledge of a ship's added resistance in waves, which has led to a need for model testing procedures, as well as for full-scale ship trials. This work has demonstrated the difficulties in accurately characterizing ship performance in a range of environmental conditions.

As the development of drag reduction technologies continues it will require improved instrumentation and testing techniques to accurately assess these technologies where the differences in the measured drag may only be 1-2%, but would still translate to a significant cost savings over the lifetime of the ship.

3. PROCEDURES

3.1 Resistance Tests

The evolution of the procedures for uncertainty analysis in measurement related to resistance tests has been overviewed.

The well-known ISO GUM (1995) is based on the Guide: Recommendation 1 (CI-1981) by the Comité International des Poids et Me-

sures (CIPM) and Recommendation INC-1 (1980) by the Working Group on the Statement of Uncertainties of the Bureau International des Poids et Mesures (BIPM). Meanwhile, the 18th ITTC Advisory Council (1984-1987) established an ad-hoc "Working Group on Validation Techniques" with the task to discuss the subject concerned numerical methods, as well as pay the attention of ITTC to the uncertainty of physical model testing. The 19th ITTC Validation Panel provided "Guideline for Uncertainty Analysis of Measurement" in Section II.3.2 of the Panel report (ITTC, 1990). They also presented excellent examples of uncertainty analysis, e.g., for resistance measurement, detailed in Section II.4.1 of the report, although, where the terminology of precision errors (random or repeatability) and bias errors (systematic or fixed) was used.

Table 3. Guides for uncertainty analysis in ITTC community before 2008

Procedure Number	Title
7.5-02-01-01	Testing and Extrapolation methods, General, Uncertainty Analysis in EFD, Uncertainty Analysis Methodology. (1999/Rev00)
7.5-02-01-02	Testing and Extrapolation Methods, General, Uncertainty Analysis in EFD, Guidelines for Resistance Towing Tank Tests. (1999/Rev00)
7.5-02-01-03	Testing and Extrapolation, General, Density and Viscosity of Water. (1999/Rev00)
7.5-02-02-01	Testing and Extrapolation Methods, Resistance, Resistance test. (2002/Rev01)
7.5-02-02-02	Resistance, Uncertainty Analysis, Example for Resistance Test. (2002/Rev01)
7.5-02-02-03	Resistance, Uncertainty Analysis Spreadsheet for Resistance Measurements. (2002/rev00)
7.5-02-02-04	Resistance, Uncertainty Analysis Spreadsheet for Speed Measurements. (2002/rev00)
7.5-02-02-05	Resistance, Uncertainty Analysis Spreadsheet for Sinkage and Trim Measurements. (2002/rev00)
7.5-02-02-06	Resistance, Uncertainty Analysis Spreadsheet for Wave Profile Measurements. (2002/rev00)
ISO GUM	Guide to the Expression of Uncertainty in Measurement. (1995) (Drafted in 1993)

Since 1999, ITTC has recommended a series of procedures/guidelines for uncertainty analysis according to the AIAA methodology, as shown in Table 3.

The 25th ITTC Specialist Committee on Uncertainty Analysis (2005-2008) revised the procedure 7.5-02-01-01 and in 2008, the 25th ITTC agreed to shift the methodology for analysis of uncertainty in measurement from the AIAA standard (symbolically by bias and precision uncertainties) to the ISO GUM methodology (symbolically by type A and type B uncertainties).

Additionally, considering there is no substantial information given by the procedure 7.5-02-01-02(1999), "General guideline for uncertainty analysis of resistance tests", the specialist committee decided to revise it as an illustrative example for application of ISO GUM into a specific kind of hydrodynamic experiments in towing tanks. This revised procedure 7.5-02-01-02 was accepted and however, finally re-numbered 7.5-02-02-02 in 2008. Logically, this re-allocation of numeration is more proper, as this procedure should be in the procedure group of 7.5-02-02 related to resistance tests. However, the procedure originally numbered 7.5-02-02-02 (2002), "Example for uncertainty analysis of resistance tests", was dropped in 2008, although it would be better to be re-numbered 7.5-02-02-02.1, as a supplement of 7.5-02-02-02 (2008). The 27th ITTC Resistance Committee decided to revise this disappearing original procedure and then suggest to recover it as newly numerated 7.5-02-02-02.1 (2014), see Table 4.

Table 4. Changes in ITTC procedures for uncertainty analysis related to resistance in 2008

Procedure Number	Title
7.5-02-01-01	Guide to the Expression of Uncertainty in Experimental Hydrodynamics. (2008/Rev01)
7.5-02-01-02	(Revised and re-numbered 7.5-02-02-02)
7.5-02-02-02	Testing and Extrapolation Methods, General Guidelines for Uncertainty Analysis in Resistance Towing tank Tests. (2008/Rev01)

In revised version of the dropped procedure 7.5-02-02-02.1 (2008), a methodology is provided that shows how ISO GUM process can applied in experimental hydrodynamics and illustrates some specific consideration that should be taken into the uncertainty analysis of resistance measurements, such as about the uncertainty of wetted surface area in resistance tests. Especially, the procedure is revised to focus on resistance measurement, and does not include the process of extrapolation, so as to avoid the existing disputes on the analysis of uncertainties or more correctly modelling assumptions related to frictional line, form factor and residuary resistance coefficient, which should be dealt with in a new procedure for uncertainty analysis of extrapolation in future.

For underwater vehicles, e.g., torpedo and submersible, the wetted surface area can usually be estimated mathematically by the tolerance of manufacture or practically measured with a systems such as a 3D Terrestrial Laser Scanner. The displacement volume of a submerged model represents the size of model and can be expressed as

$$\nabla \propto L \cdot B \cdot H \tag{1}$$

and the wetted surface area can be expressed as,

$$S \propto \left[(\nabla)^{1/3}\right]^2 \tag{2}$$

where, L is the characteristic length, B the width and H the height of model. The relative tolerance of displacement volume can be estimated as

$$\left(\frac{\delta\nabla}{\nabla}\right)^2 \approx \left(\frac{\delta L}{L}\right)^2 + \left(\frac{\delta B}{B}\right)^2 + \left(\frac{\delta H}{H}\right)^2 \tag{3}$$

and then the relative uncertainty of displacement volume can be evaluated by combination of the uncertainties of length, width and height,

$$u'_{\nabla} \equiv \frac{u_{\nabla}}{\nabla} \approx \sqrt{(u'_L)^2 + (u'_B)^2 + (u'_H)^2} \tag{4}$$

where, u denotes the standard uncertainty. Thereafter, the uncertainty of wetted surface area can be estimated as

$$u'_S \equiv \frac{u_S}{S} \approx \left(u'_\nabla\right)^{2/3} \tag{5}$$

For surface vessels, the size of its underwater part is determined by its weight (displacement mass, Δ),

$$\nabla = \frac{\Delta}{\rho_{water}} \tag{6}$$

Then, its uncertainty can be estimated by

$$u'_\nabla \equiv \frac{u_\nabla}{\nabla} \approx \sqrt{\left(u'_\Delta\right)^2 + \left(u'_{\rho\_water}\right)^2} \tag{7}$$

And the uncertainty of wetted surface area can be calculated by Equation 5.

On the other hand, all the procedures as listed in Table 2 for uncertainty analysis of resistance tests seem to focus mainly on interpreting the test results to the users of CFD simulation and are too complicated to be practical or even useful to routine tests in towing tank. They are seen to be much too mathematical rather than of practical engineering use in regular towing tank tests.

The 27th ITTC Resistance Committee performed uncertainty analysis for a real example of a new series of resistance tests of DTMB 5415 model and found that the dominant components of uncertainty are of dynamometer accuracy (evaluated by calibration) and repeatability (estimated by repeat tests), as shown in Table 5 and Eq.8,

$$\begin{aligned} u'_C &= \sqrt{\left(u'_1\right)^2 + \left(u'_2\right)^2 + \left(u'_3\right)^2 + \left(u'_4\right)^2 + \left(u'_5\right)^2} \\ &\approx \sqrt{\left(u'_2\right)^2 + \left(u'_5\right)^2} \\ &= \sqrt{\left(u'_{\text{dynamometer}}\right)^2 + \left(u'_{\text{repeatability}}\right)^2} \end{aligned} \tag{8}$$

This is in agreement with experiences in well-controlled commercial towing tanks. Therefore, the spreadsheet for resistance measurement (the procedure 7.5-02-02-03) is not necessary or even not useful for routine practice of commercial tests, because the total/combined uncertainty in resistance can be estimated simply by RSS (Root-Sum-Square) of that of dynamometer calibration and repeat tests as in Equation 8, although such a spreadsheet may be used in investigation of UA method or for detailed comparison of intra- and inter-laboratory tests.

Table 5. Example of uncertainty analysis in resistance measurement of DTMB 5415 model

Component of Uncertainty in R_T	Type	Uncertainty Component in R_T (Fr=0.28)
Wetted Surface Area	B	u'_1 = 0.035 %
Dynamometer (v=32)	A	u'_2 = 0.19 %
Towing Speed	B	u'_3 = 0.067 %
Water Temperature	B	u'_4 = 0.024 %
Repeatability (N=9)	A	u'_5 = 0.45 %
Combined uncertainty for single measurement		u'_C = 0.49 %
Expanded uncertainty for single measurement (k_P=2)		U'_P = 0.98 %

Furthermore, the uncertainty propagated from towing speed into resistance can usually be considered negligible when the speed can be controlled with the accuracy recommended by the ITTC procedure 7.5-02-02-01. Therefore, the spreadsheet by the procedure 7.5-02-02-04 (2002) is not needed for routine tests.

The value of resistance is closely correlated to the running sinkage and trim, but there is no

analytical relation between resistance and its corresponding sinkage and trim. If special attention is given to the measurement of sinkage and trim, the detailed analysis as with the spreadsheet in the procedure 7.5-02-02-05 (2002) may be needed.

Finally, the measurement of wave profile is quite different from that of resistance. Before developing a procedure for uncertainty analysis, a detailed procedure should be recommended for testing of wave profile measurement itself.

It is suggested that all the spreadsheets in the procedures 7.5-02-02-03~06 (2002) can be dropped or if needed, revised in future and additionally, when repeat tests are performed to obtain the mean as measured and evaluate the uncertainty of repeatability, the outlier detection will be included in the spreadsheets.

4. WORLD WIDE CAMPAIGN

The world wide campaign has occupied the resistance committee since the 24th ITTC. No new submissions have been made to the committee since the 26th ITTC. The analysis presented uses the available data to draw conclusions about inter-tank bias. A new spreadsheet based analysis tool was developed to draw together all the data for comparative purposes. Although it is disappointing not to be able to fully exploit all the tests conducted by the many tanks who participated testing the small and large geosim models unless the data is submitted there is little that can be done. Similarly where there are ambiguities in the data submitted due to the double blind nature of the testing these are impossible to resolve.

4.1 Inter-laboratory comparison

The comparison of test data from a total of 11 towing tanks for the large model of DTMB 5415 has been performed, as in what appears to be a mistake the data from No.10 tank is identical to that from No. 4.

The large model, denoted as Geosim A, used in the ITTC worldwide comparative tests is the CEHIPAR model 2716, a wooden geosim of the model DTMB 5415, with Lpp of 5.72 m, draft of 0.248 m in calm water without trim, displacement volume of 549 m3 (ITTC, 2005), corresponding to a scale of 24.824. The nominal wetted surface area of 4.786 m2 (Olivieri et al, 2001) is adopted in expressing the total resistance coefficient (CT).

As prescribed by the ITTC comparative tests, there would be used 9 repeat tests at each speed in each of towing tanks to perform statistical analysis. All the total resistance measurements in a specific tank are corrected to the nominal speed (Fr=0.1, 0.28 and 0.41) and converted to the nominal temperature of fresh water 15 degrees Celsius before any statistical analysis is made.

The means of total resistance coefficients from those repeat tests in each tank are given in Table 6. Such means can be regarded as the best measurement in each towing tank. The experimental standard deviation (*StDev*) of tests in each tank is also presented. Such standard deviations can be used to estimate the uncertainties of repeatability of measurement in each towing tank.

Table 6. Statistical analysis of resistance measurement in comparative tests of the large DTMB 5415 model in 11 towing tanks

Tank No.	$C_T(10^{-3})$_**15deg**_Fresh Water of Large Model (5.72m)_DTMB 5415_S=4.786m^2					
	***Fr* =0.1**		***Fr* =0.28**		***Fr* =0.41**	
	Mean	*StDev*	Mean	*StDev*	Mean	*StDev*
# 1	3.956	1.2%	4.156	0.2%	6.429	0.2%
# 2	3.917	1.6%	4.160	0.5%	6.497	0.5%
# 3	4.007	0.9%	4.216	0.2%	6.536	0.2%
# 4	4.306	3.6%	4.270	1.8%	6.587	1.9%
# 5	4.008	1.2%	4.248	0.4%	6.617	0.3%
# 6	3.918	1.1%	4.234	0.6%	6.639	0.3%
# 7	N/A		4.263	0.4%	6.480	0.5%
# 8	3.959	0.5%	4.166	0.5%	6.336	0.8%
# 9	4.001	1.9%	4.216	0.7%	6.590	1.9%
# 10	(#4)					
# 11	3.989	1.1%	4.190	0.4%	6.412	0.2%
# 12	4.019	2.3%	4.203	0.7%	6.368	0.7%
Averaged after outliers (in RED) ticked out						
Baseline	3.975	0.98%	4.211	0.96%	6.499	1.6%

Before any statistical analysis, a practical approach to detect outlier is suggested for intra-laboratory comparison as the following steps:

Step 1: Calculate the mean (R_0) and standard deviation (S_0) of 9 repeat tests,

$$R_0 = \frac{1}{N}\sum_i R_i \qquad (i = 1, N) \tag{9}$$

$$S_0 = \sqrt{\frac{1}{N-1}\sum_i (R_i - R_0)^2} \qquad (i = 1, N) \tag{10}$$

Step 2: Judge if there is any test result outside the scattering band of double deviation,

$$\left|R_i - R_0\right| \le 2 \cdot S_0 \quad ? \qquad (i = 1, N) \tag{11}$$

Step 3: If no test is outside the band, no outlier exists. If the kth test is outside the "double" band, it will be doubted as an outlier. Tick it out and calculate the mean (R_*) and standard deviation (S_*) of the repeat tests again, excluding the kth test.

Step 4: Judge if the kth test is outside the scattering band of triple deviation,

$$\left|R_k - R_*\right| \le 3 \cdot S_* \quad ? \tag{12}$$

Step 5: If the kth test is outside the "triple" band, its measurement can be considered as an outlier and then the mean R_* and standard deviation S_* are adopted as statistic parameters of repeat tests. Otherwise, no outlier is detected and the mean R_0 and standard deviation S_0 of repeat tests are used.

For inter-laboratory comparison, the average of measurement means of 11 towing tanks can be considered as a kind of baseline.

When averaging the means of tests in 11 tanks, the detection of outlier can be performed following the above steps. The statistical analysis and corresponding results are shown in Figures 11-13 and given in Table 7. These deviations are kind of measure for the facility bias. It is interesting to note that the scattering of data between towing tanks is much larger at speed of *Fr*=0.41 than that of *Fr*=0.1 and *Fr*=0.28.

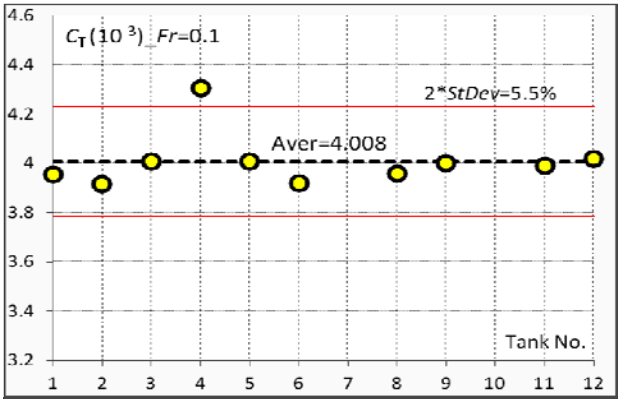

Figure 11a. Statistical analysis for means of total resistance coefficients of 10 tanks (*Fr*=0.1/including an outlier)

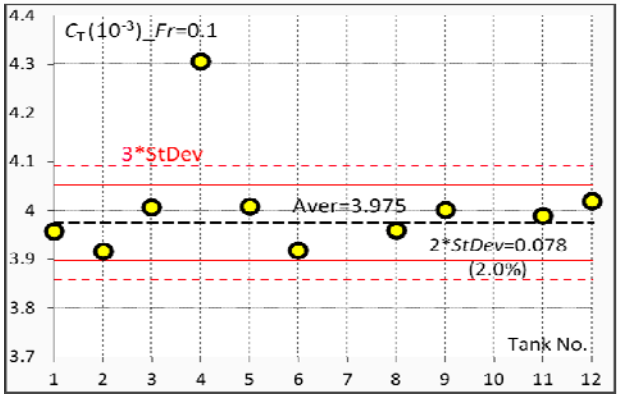

Figure 11b. Statistical analysis for means of total resistance coefficients of 10 tanks (*Fr*=0.1/excluding outlier)

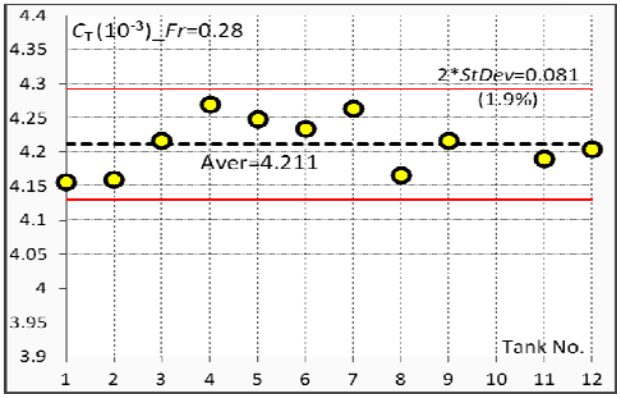

Figure 12. Statistical analysis for means of total resistance coefficients of 11 tanks (*Fr*=0.28, no outlier)

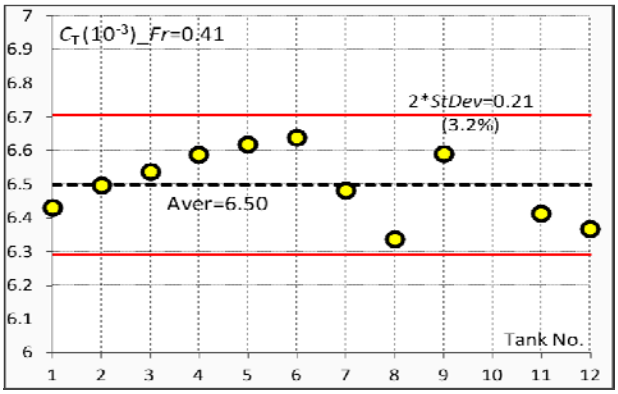

Figure 13. Statistical analysis for means of total resistance coefficients of 11 tanks (*Fr*=0.41, no outlier)

The normalized deviations of means of resistance in each tank from the overall average of all tanks are summarized in Figure 14 and it shown that almost 95% of the means are within the scattering band of 2% of the overall average, when the outlier is excluded.

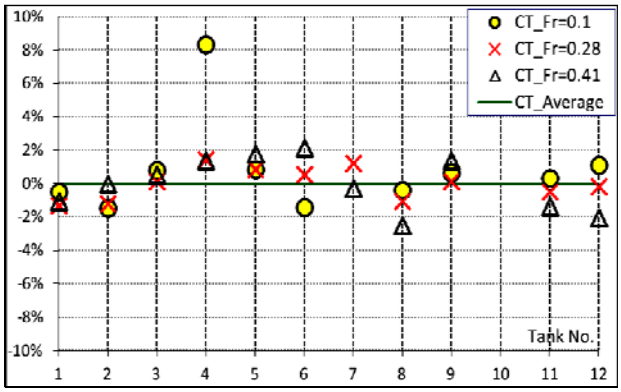

Figure 14. Scattering of means of resistance by 11 towing tanks in comparative tests of the large DTMB 5415 model

The measurements of running sinkage and trim would present more information to intra- and inter-laboratory comparison of resistance tests. For intra-laboratory comparison, the statistical analysis for sinkage and trim from repeat tests in each towing tank is given in Table 7-9. Obviously, the scattering of resistance is not closely correlated to that of sinkage.

Table 7. Statistical analysis of running sinkage and trim measurement in comparative tests of the large DTMB 5415 model (*Fr*=0.1)

***Fr* =0.1**	$C_T(10^{-3})$_**15deg**_Fresh Water of Large Model (5.72m)_DTMB 5415_S=4.786m^2					
Tank No.	**Resistance C_T**		**Sinkage** (mm)		**Trim** (Deg)	
	Mean	*StDev*	Mean	*StDev*	Mean	*StDev*
# 1	3.956	1.2%	-1.64	0.31	-0.015	0.002
# 2	3.917	1.6%	-1.05	0.40	-0.008	0.006
# 3	4.007	0.9%	-1.19	0.08	-0.012	0.001
# 4	4.306	3.6%	-0.85	0.24	-0.018	0.011
# 5	4.008	1.2%	N/A			
# 6	3.918	1.1%	N/A			
# 7	N/A		N/A			
# 8	3.959	0.5%	-1.30	0.03	-0.012	0.000
# 9	4.001	1.9%	N/A			
# 10	(#4)					
# 11	3.989	1.1%	-0.89	0.31	-0.014	0.001
# 12	4.019	2.3%	N/A			
Averaged after outliers (in RED) ticked out						
Average (Baseline)	**3.975**	0.98%	**-1.05**	0.19	**-0.013**	0.003

Table 8. Statistical analysis of running sinkage and trim measurement in comparative tests of the large DTMB 5415 model (*Fr*=0.28)

***Fr* =0.28**	$C_T(10^{-3})$_**15deg**_Fresh Water of Large Model (5.72m)_DTMB 5415_S=4.786m^2					
Tank No.	**Resistance C_T**		**Sinkage** (mm)		**Trim** (Deg)	
	Mean	StDev	Mean	StDev	Mean	StDev
# 1	4.156	0.2%	-10.95	0.29	-0.113	0.002
# 2	4.160	0.5%	-10.75	0.43	-0.103	0.005
# 3	4.216	0.2%	-10.49	0.11	-0.102	0.002
# 4	4.270	1.8%	-10.39	0.30	-0.111	0.009
# 5	4.248	0.4%	-9.21	0.14	-0.098	0.003
# 6	4.234	0.6%	-12.59	0.19	-0.118	0.003
# 7	4.263	0.4%	-10.23	0.16	-0.104	0.002
# 8	4.166	0.5%	-10.34	0.10	-0.101	0.001
# 9	4.216	0.7%	-10.32	0.35	-0.097	0.004
# 10	(#4)					
# 11	4.190	0.4%	-10.05	0.30	-0.015	0.004
# 12	4.203	0.7%	-9.35	0.15	-0.016	0.002
Averaged after outliers (in RED) ticked out						
Average (Baseline)	**4.211**	0.96 %	**-10.21**	0.55	**-0.104**	0.005

Table 9. Statistical analysis of running sinkage and trim measurement in comparative tests of the large DTMB 5415 model (*Fr*=0.41)

***Fr* =0.41**	$C_T(10^{-3})$_**15deg**_Fresh Water of Large Model (5.72m)_DTMB 5415_S=4.786m^2					
Tank No.	**Resistance C_T**		**Sinkage** (mm)		**Trim** (Deg)	
	Mean	StDev	Mean	StDev	Mean	StDev
# 1	6.429	0.2%	-27.35	0.25	0.335	0.012
# 2	6.497	0.5%	-26.30	0.33	0.373	0.004
# 3	6.536	0.2%	-26.67	0.16	0.430	0.004
# 4	6.587	1.9%	-25.96	0.51	0.415	0.019
# 5	6.617	0.3%	-22.52	0.12	0.361	0.005
# 6	6.639	0.3%	-29.45	0.28	0.535	0.009
# 7	6.480	0.5%	-24.40	0.16	0.403	0.009
# 8	6.336	0.8%	-25.21	0.07	0.367	0.005
# 9	6.590	1.9%	N/A			
# 10	(#4)					
# 11	6.412	0.2%	-25.24	0.08	0.378	0.006
# 12	6.368	0.7%	-24.39	0.20	0.352	0.004
Averaged after outliers (in RED) ticked out						
Average (Baseline)	**6.499**	1.6%	**-25.34**	1.45	**0.379**	0.031

For intra-laboratory comparison, the statistical analysis for means of sinkage and trim from repeat tests in each towing tank is shown in Figures 15-17 and also presented in Table 7-9. The scattering of resistance is not closely correlated to that of sinkage, either, as shown in Figure 18.

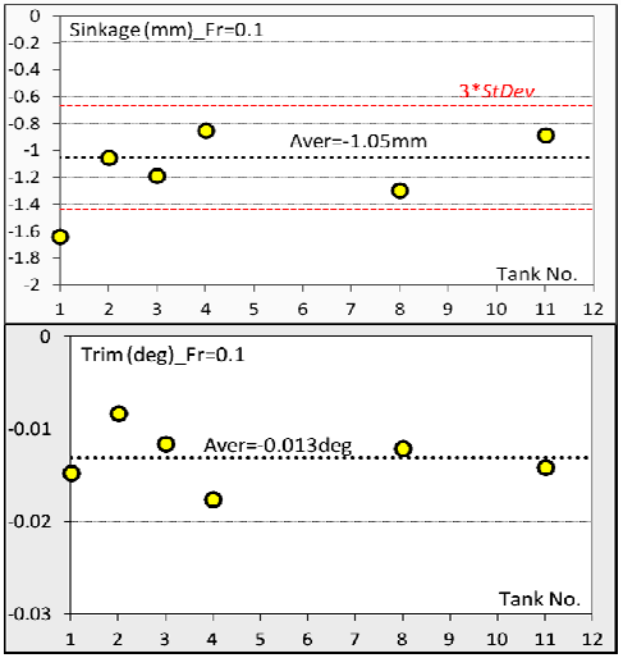

Figure 15. Statistical analysis of running sinkage and trim measurement in comparative tests of the large DTMB 5415 model (*Fr*=0.1)

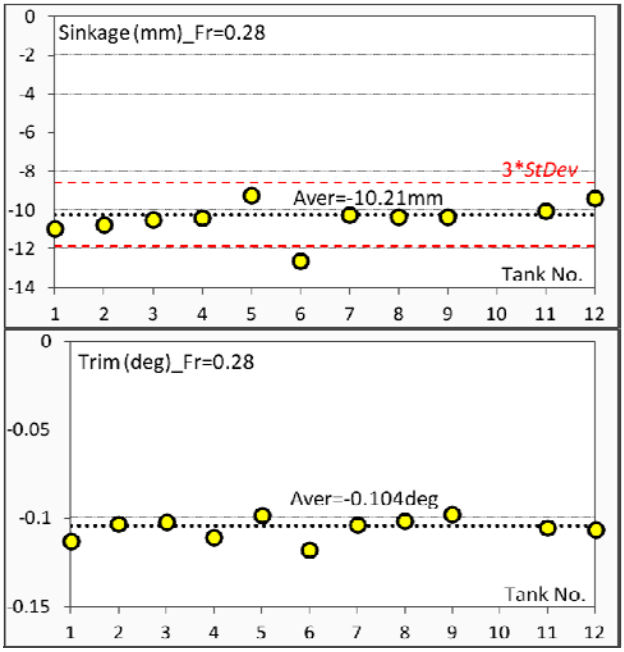

Figure 16. Statistical analysis of running sinkage and trim measurement in comparative tests of the large DTMB 5415 model (*Fr*=0.28)

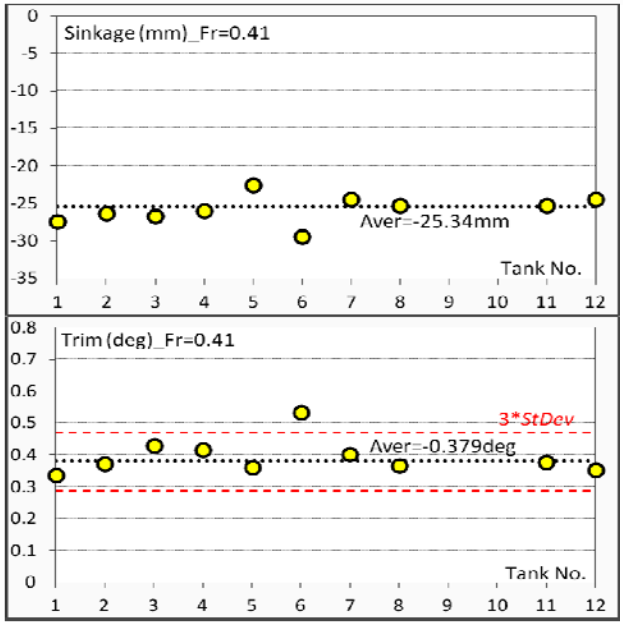

Figure 17. Statistical analysis of running sinkage and trim measurement in comparative tests of the large DTMB 5415 model (*Fr*=0.41)

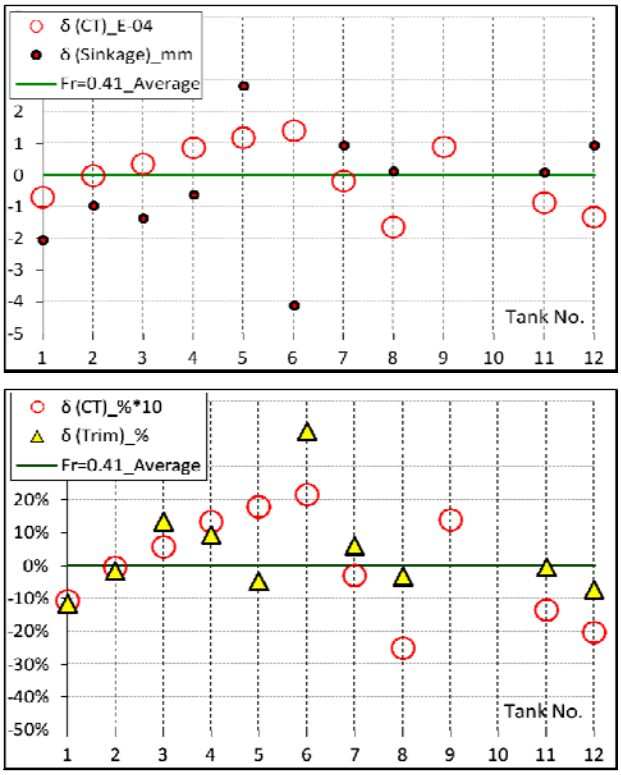

Figure 18. Correlation analysis of resistance to sinkage and trim measurement in comparative tests of the large DTMB 5415 model (*Fr*=0.41)

4.2 Wave Resistance Evaluation from Worldwide Campaign

Tests were done during the 24th, 25th and 26th ITTC periods. In the 24th ITTC, 20 institutions from 15 countries have been carried on the tests while in the 25th ITTC, 35 institutions from 19 countries have been participants. In the last 26th ITTC period, 41 institutions from 20 countries have been carried on the tests.

During the tests two geosims of the DTMB 5415 Combatant with 5.720 and 3.048 meters length have been used, see Table 10. Test Froude numbers are selected as 0.1, 0.28 and 0.41 and carried on 4 different days and 10 runs each set.

Table 10. Hull geometric parameters

L_{PP} (m)	5.720
B_{WL}(m)	0.724
T(m)	0.402
∇(m³)	0.842
S (m²)	4.8273

The purpose of the resistance test is to produce data for the temperature-corrected resistance coefficient. The total measured resistance values have been given with the file system. Therefore,

$$C_{TM} = \frac{R_{TM}}{\frac{1}{2}\rho_M S_M V_M^2} \tag{13}$$

The residuary resistance of the model is calculated from the model resistance tests taking the form factor equals to k=0.15 (Stern et al, 2010) which is to be independent of scale and speed. The residuary resistance can therefore be calculated as:

$$C_R = C_{TM} - C_{FM}(1+k) \tag{14}$$

where CFM is derived from the ITTC – 1957 correlation line.

An Excel macro based spreadsheet is developed for the evaluation of wave resistance. The extreme values of maximum and minimum of residuary resistance of two models are given in Table 11.

Table 11. Maximum and minimum values of residuary resistance

Fr	LARGE MODEL (5.72m)		SMALL MODEL (3.048m)	
	Min C_R*1000	Max.C_R*1000	Min C_R*1000	Max.C_R*1000
0.10	-19.0788	20.84345	-18.79000	23.66018
0.28	-1.8363	3.5725	-2.43352	4.82622
0.41	1.2535	5.6700	-0.33806	6.75376

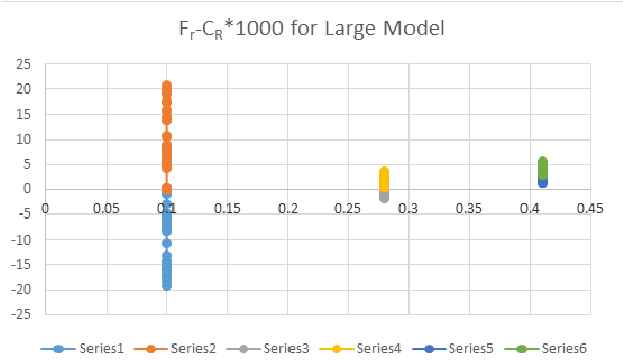

Figure 19. Distribution of maximum and minimum values of residuary resistance for the Large Model.

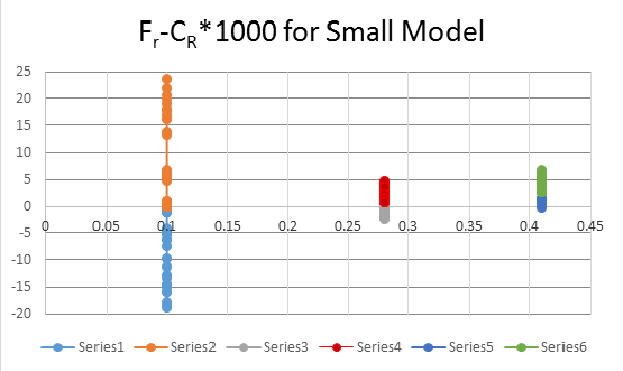

Figure 20. Distribution of maximum and minimum values of residuary resistance for the Small Model.

Figures 19 and 20 show the distribution of maximum and minimum wave resistance values for each institute. The diversity in residuary resistance is quite high for the Fr= 0.1 when comparing with the others due to the measurement sensitivity is poor in the low speed range. Additionally, the spread of in resistance values is higher for the small model when compared to the large one for the Froude numbers 0.28 and 0.41.

Negative wave resistance values exist in both models for the Froude Number 0.28 due to the definition of form factor. Negative residuary resistance values still exist in the small

model for the Froude Number 0.41. Such values suggest that selecting a fixed value of form factor valid for all Fn is incorrect. Indeed for dynamic hull with significant amounts of sinkage and trim a Fn dependency is to be expected and could be resolved through use of longitudinal wave cuts for measuring wave resistance, (Molland et al, 2011).

The usefulness of the spreadsheet based approach and other studies can be carried out using suitable macro functions in the future as it is able to access the whole database.

4.3 Comparison with variation from Gothenburg 2010 study

As previously reported (ITTC, 2011b) the same hull DTMB 5415 tested at two scales in the ITTC world wide campaign was one of the test cases (3.1a,3.1b and 3.2) for the Gothenburg 2010 CFD Workshop (Larrson *et al*, 2014). Figure 21 shows the % variability for the total resistance coefficient for all the CFD values as a function of computational mesh size. The benchmark value for DTMB5415 is taken as the value from a single experimental source. In looking at the variability in the CFD data especially noting the differences between fixed and free to trim calculations, it can be seen that for the vast majority of the CFD results even for the smallest mesh cases lie within 5% of the mean.

The accompanying statistical analysis for the DTMB hull extracted here as Table 12 quantifies values with mean differences from the single experimental test case varying between 0.1% (free at Fn=0.28) and 4.3% (free at 0.41), In comparing these values with those presented for the large model which had a standard deviation of 1% from the mean, although the CFD still has a larger variability, with larger mesh calculations the uncertainty is approaching that of the general capability of towing tanks to measure resistance. Another point worth emphasising is that the Gothenburg workshop used test data from INSEAN (Case 3.1 fixed , large model Fn=0.28), IIHR (Case 3.1b fixed, small model Fn=0.28) and INSEAN (Case 3.2, free to sink and trim, large model Fn=0.28,0.41). The majority of the data in Larrson *et al* (2014) is presented as a percentage difference from the experimental value. For case 3.1a for the large model as shown in Table 8 the World Wide Campaign (WWC) mean value of C_T is 4.21×10^{-3}.although comparable with the value of 4.23×10^{-3} shown in Fig. 5.24 of Zou and Larrson(2014). This change increases the error from 2.6% to 3.1% although the WWC was a different physical model. The comparable change for the more realistic free model (case 3.2) is from 0.1%D to 0.6%D.

It is worth noting that the uncertainty with computing free sinkage and trim appears already to be comparable with the capabilities of tanks to measure these quantities to a common datum. One useful facet not originally included in the values of sinkage and trim was the influence on uncertainty on the level of the IIHR rails, (Larrson *et al*, 2014, 53-64). After the original presentation of the data it was found that there were significant variation in both rails in the IIHR towing tank. These were subsequently re-levelled increasing the overall experimental uncertainty in sinkage for instance from a maximum measured variation of 1.29mm on the east rail to 0.462mm.

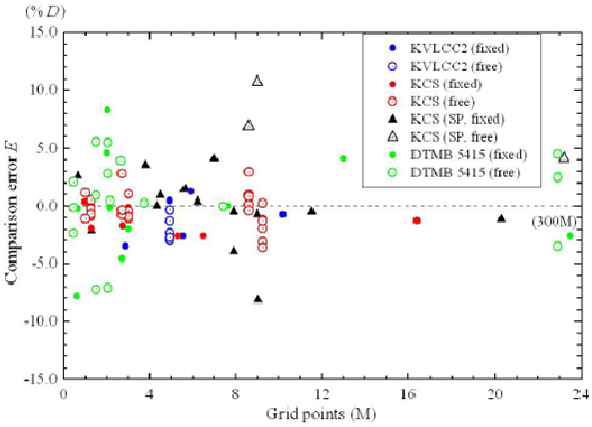

Figure 21. Variation in Resistance Coefficient with mesh for all Gothenburg 2010 calm water resistance test cases, including worldwide campaign hull DTMB5415,

Table 12 Gothenburg 2010 Calm water resistance CFD results for DTMB5416 test cases

Case	Fn	%E	σ %	No. of Submissions
3.1a Fixed S &T	0.28	2.5	5.3	11
3.1b Fixed S & T	0.28	-2.6	4.4	5
3.2 Free	0.138	-2.8	4.4	5
	0.28	0.1	2.1	6
	0.41	4.3	1.4	5

4.4 Recommendations for the World Wide Campaign

The worldwide campaign data should be made available via new ITTC website. The previous committee has provided an easily used database for additional studies. Further analysis was conducted by the committee and has shown some greater understanding. No new data was received. We suggest an approach for inter tank bias comparison, established a base line by removing 'outliers' and make accessible the whole database via new ITTC website and will provide a searchable spreadsheet for use when looking at all data. A comparison is made with the corresponding data from the CFD analysis from Gothenburg 2010.

For future such campaigns, the double blind although a good idea in reality was too much of challenge. The inability to resolve ambiguities in submission, despite the prescriptive spreadsheet based uncertainty procedures (7.5-02-02-03 to 7.5-02-2.06) and the failure of many towing tanks to submit the analysed data severely restricted the size of the data set for both large and small models. Similarly the challenge of moving models between countries and the possibility of damage due to transit could very well have introduced its own age related bias. Any future such activity led by the ITTC should consider following an open approach to ensure the collective community of expertise can ensure data collected is always to a high standard. Questions that are as yet not possible to resolve are whether the dominant bias is associated with tank blockage or if as in the IIHR tests it is the lack of levelness in the rails which causes the problems with the sinkage and trim comparisons.

5. SURFACE ROUGHNESS

5.1 Introduction

This section summarizes the state of art in hull surface roughness of actual ship and its influence on the roughness allowance (ΔC_F), including experimental and numerical approaches.

5.2 Measurement and evaluation of roughness

For the measurement of roughness of actual hull surface, the BMT Sea Tech Hull Roughness Analyser (a stylus instrument with a surface probe) is used in many shipyards as the standard measurement tool. The hull roughness is normally measured in the way that the hull is divided into 10 equal sections with 10 measurements each, 5 on the port side and 5 on the starboard side. A total of 50 readings are taken on each side, 30 on the vertical sides and 20 on the flats. From the 100 measuring locations, the average hull roughness is calculated (ITTC 2011).

In ISO-4287:1996, various roughness parameters are defined. Surface roughness in general is a measure of the texture of a surface, and this is calculated on a profile or on a surface. Profile roughness parameters (Ra, Rq….) are more common whereas area roughness parameters (Sa, Sq,….) give more significant values.

There are many different roughness parameters in use, but Rz, is a useful parameter because it can consider as the BMT roughness parameters. The definition of Rz in 50 mm evaluation length is similar to definition of BMT roughness, and its value is almost same. (Mieno, 2012).

On the other hand, roughness measurements on ship models are carried out at few model basins (e.g. MARIN, SSPA), but the results of the measurements are used for quality assurance and not for further investigation. Most of the model basins do not measure the roughness of the model's hull.

5.3 Experimental approach of roughness influence

In order to clarify correlation between properties of coatings on ship hull surface and frictional resistance, experimental studies were carried out by Tanaka et al. (2003), Weinell et al. (2003), and Mieno (2012). A rotating cylinder type dynamometer is used to measure frictional resistance of coatings at higher Reynolds number flow similar to that around a real ship. Measuring the frictional resistance and change of roughness of cylinders coated with self-polishing type paint or water repellent paints, correlation between properties of coating and frictional resistance can be investigated. Further, a simple method based on these experimental results like that shown in Figure 22 can estimate the frictional resistance acting on the surface of the actual ship hull.

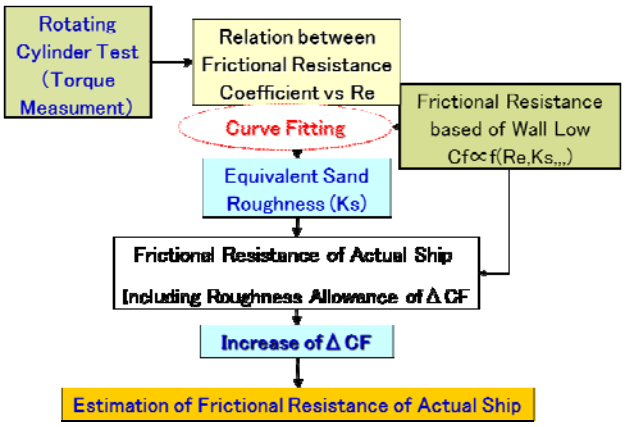

Figure 22. Schematic flow of roughness allowance estimation by rotating cylinder method.

Tanaka et al (2003) proposed roughness allowance estimation method based on the results of rotating cylinder experiments. Under the assumptions that the flow around the rotating cylinder around becomes turbulent and wall law is established near surface of the cylinder near the surface, velocity profile in boundary layer is as follows.

$$u^* = \frac{1}{\kappa} \ln y^+ + B - \Delta B \qquad (15)$$

Estimating roughness function ΔB, frictional resistance including influence of roughness can be easily obtained by boundary layer calculation. In Figure 23, it is shown an example of correlation between surface roughness and frictional resistance.

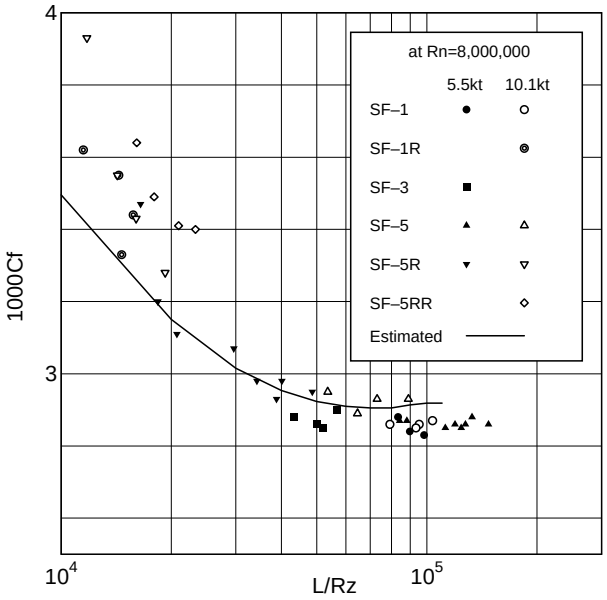

Figure 23. Correlation between surface roughness and resistance coefficient (Tanaka 2003).

When equivalent sand roughness Ks of an actual ship hull is obtained, roughness allowance ΔCF can be estimated by various expressions of frictional resistance. An example of estimated roughness allowance by White's formula (White, 1991) is shown in Figure 24.

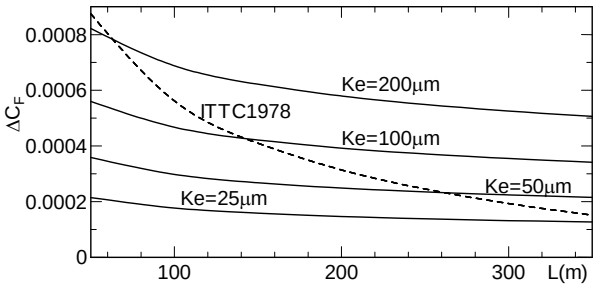

Figure 24. Example of estimated roughness allowance for actual ship (Tanaka 2003).

The rotating cylinder method is used in order to investigate the effect of damaged hull surface, newly developed paint performance. Weinell et al. (2003) carried out the rotating cylinder tests to investigate the effect of roughness on the frictional drag. One smooth cylinder and two sand roughened cylinders are used for reference, seven roughened cylinders are investigated. In the experiment, torque is measured. Further, ageing effect for fiber and non-fiber containing paints are also examined. Also roughness of simulated weld seam and simulated paint remain are also investigated. With respect to frictional drag, the contribution from a modern self-smoothing antifouling or silicone based fouling-release paint is negligible compared to the contribution from irregularities found on ship's hull. In the investigated range of roughness, micro-roughness was found to be much more important than macro-roughness. On the other hand, large-scale irregularities were found to be even more important than both micro-and macro-roughness.

Mieno (2012) investigated the influence of various roughness parameters to frictional resistance increase. In this study the influence of the surface roughness on the friction was measured using rotating cylinder, and roughness was measured with a Laser displacement meter and the surface parameters were investi-

gated by the JIS B 06015 method (similar to ISO-4287). Roughness of an actual ship hull surface was measured by replicar method. The Friction Increasing Ratio FIR(%) is defined in Equation (16). T is equal to the torque measured using a painted cylinder and T_0 is the torque measured on a smooth surface cylinder.

$$FIR(\%) = \frac{T - T_0}{T_0} \times 100 \qquad (16)$$

Relation between R_z and FIR is shown as a graph in Figure 25. Dry spray (DS) are plotted as the △ symbol, conventional self-polishing coating (C_SPC) as the ◇symbol, new generation self-polishing coating (N_SPC) as the ○ symbol, foul release coating (FRC) as the □ symbol. Friction increasing was observed according to increasing of R_z. Even at the same R_z value, FIR differences are observed between FRC, N_SPC, C_SPC and DS. Relation between S_m and FIR is shown in Figure 26. S_m of DS ranges from 2000 to 3000 micron and FIR is more than 25%. S_m of C_SPC ranges from 3000 to 4500 micron of N_SPC from 4000 to 7000 micron and of FRC S_m is more than 8000 micron. FIR for FRC and N_SPC is less than 2%. A lower S_m-value tends to increase FIR more than a higher value. Sasajima (1965) reported a correlation between the squared height parameter divided by wavelength as H^2/λ and the friction coefficient. When R_z is considered as H, and also S_m is considered as λ, there should be a correlation between FIR and R_z^2/S_m.

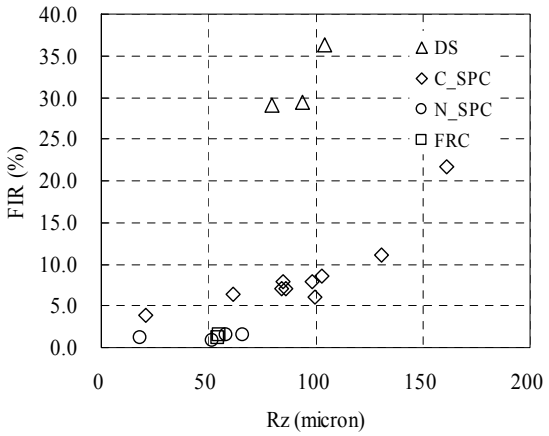

Figure 25. Relation between R_z and FIR (Mieno 2012)

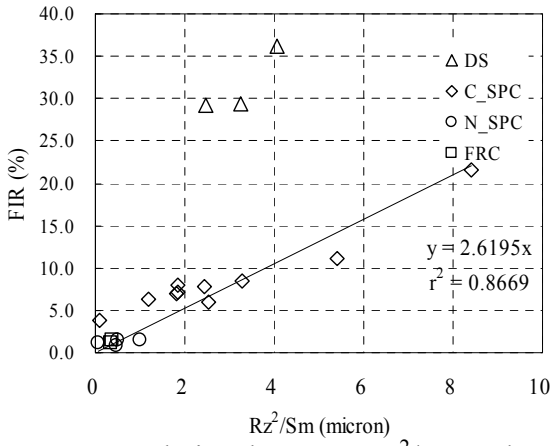

Figure 26. Relation between R_z^2/S_m and FIR (Mieno 2012)

As a new experimental technique using a flat plate, Kawashima (2012) has proposed a new experimental method shown in Figure 27. Aiming to clarify the relationship between friction resistance and roughness parameter (height, period, slope, etc.), the authors carried out tank tests of flat plates that have various types of roughness by painting. According to the results of the tank test, frictional resistance increase becomes smaller as roughness height length ration H/L becomes larger.

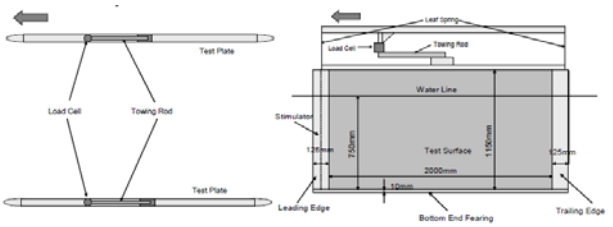

Figure 27. Schematic view of measurement system (Kawashima, 2012).

5.4 Theoretical and numerical approach of roughness influence

A new theoretical friction factor model for fully developed turbulent internal flows of smooth and rough pipes and channels has been developed by using a new velocity profile, which is a combination of logarithmic and power law profiles (Atkan et al, 2009). The proposed equation is explicit function of Reynolds number and relative roughness. Constants in the derived equation for the friction factor are given by experimental data. The formula recovers Prandtl's law of friction for smooth pipes well. The model also shows good correlation with the available data for turbulent flows in rough pipes for wide ranges of Reynolds number and surface roughness covering the entire Moody chart. The maximum relative error between the published experimental friction factors and those calculated from the developed equation was found to be less than 3%, and the proposed relationship agrees with the Blasius relationship for low Reynolds numbers to within 1%.

Considering roughness influence, Katsui et al. (2011) proposed a new flat plate friction formula for wide Reynolds number range based on momentum-integral equation and Coles' wall-wake law. The flat plate frictional coefficient is evaluated by solving a differential equation introduced White's roughness function. Roughness allowance ΔC_F by surface roughness is dependent upon roughness height non-dimensionalized by plate length and Reynolds number. It is possible to evaluate full scale ship resistance increase caused on surface roughness with the presented method. To estimate ΔC_F easily, ΔC_F formula approximated with function of non-dimensional roughness height is also presented in Figure 28.

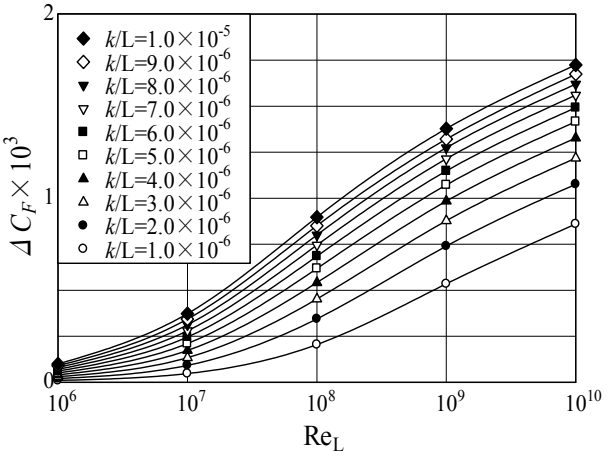

Figure 28. Added frictional resistance due to surface roughness (Katsui et al, 2011).

Eça and Hoekstra (2010) reported the effects of hull roughness on viscous flows around ships. These effects are computed by replacing the typically non-uniform roughness of the hull surface by a uniform sand roughness. The calculations are performed with the RANS-code PARNASSOS using the SST k−ω model. No wall functions are applied, and the roughness effect is introduced via a change in the ω wall boundary condition. For a tanker, a container ship and a car carrier, the flow is computed at model and full scale Reynolds numbers for sand-grain roughness heights ranging from 0 (smooth wall) to 300 μm. Each case is computed on six nearly geometrically similar grids to allow a fair estimate of the numerical uncertainty. The results shown, in Figure 29, confirm that an increase of the roughness height leads to an increment of the friction and pressure resis-

tance coefficients and the wake fraction. It is clear from the data that there is a significant scale effect, depending not only on the global Reynolds number (based on the ship length) but also on the roughness Reynolds number (based on the roughness height). The combination of the effects observed for C_F and C_P is reflected in the viscous resistance coefficient, C_V. Since C_F is dominant, the behavior of C_V is similar to that observed for C_F. The roughness height does not affect only the near-wall flow. The wake field at the propeller plane is also clearly influenced by h_R. The thickness of the "boundary-layer" and the mean wake fraction grow with the increase of h_R.

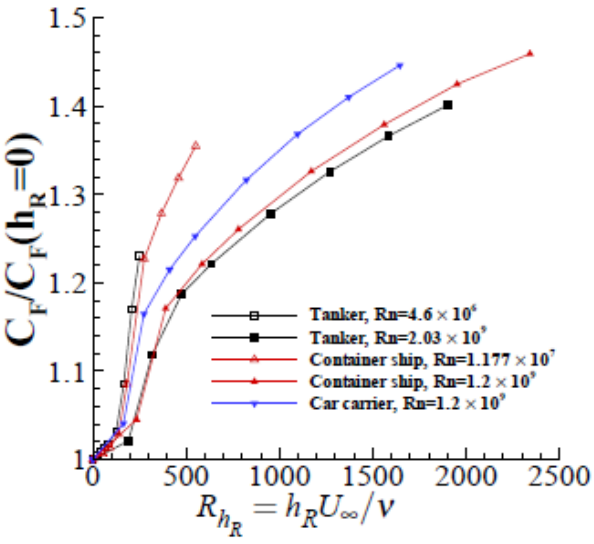

Figure 29. Ratio between friction resistance coefficients predicted with and without sand-grain roughness.

As the first step toward the flow simulation of a full scale ship with hull surface roughness, Hino (2012) computed simple 2-D channel flows and flat plate flows using the current turbulence models with roughness effect. The results are compared between a smooth wall and a rough wall and the level of applicability of the current roughness models is examined. Flow computations in a 2-D channel and around a flat plate with and without surface roughness are carried out in order to examine the applicability of the current roughness models in a turbulence closure. 2-D Channel test cases show that κ-ω based roughness model is more robust than SA based model, though both models can simulate effects of sand-grain roughness fairly well. The flat plate simulations also reproduce a reasonable behaviour of frictional resistance increase by the roughness effect. For applications to full scale ship flows with a surface roughness, the extension of the current roughness model is required, since the roughness distribution is supposed to be not uniform in the paint surface of an actual ship as shown in Figure 30.

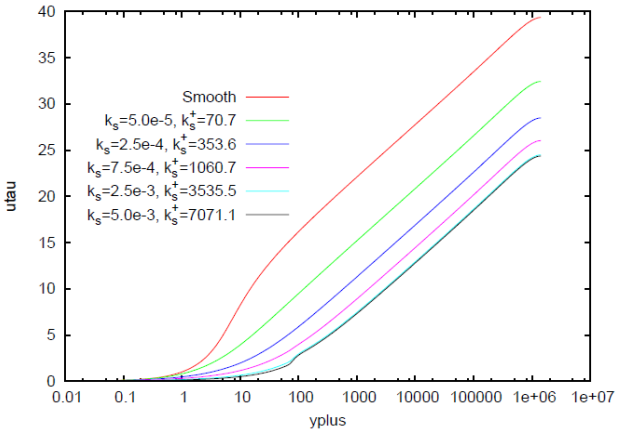

Figure 30. Logarithmic plots of velocity profiles by SST model at Rn ≈ 108 (Hino, 2012).

5.5 Conclusions

ISO-4287 definitions of roughness, which are widely used in industry, are possible to represent various characteristics of roughness. On the other hand, measurement with BMT roughness analyser is general in many shipyards, but it seems to be difficult to understand various characteristics of roughness by the device. Because Reduction of frictional resistance is the essential task for energy saving, it is expected that new types of paints for this purpose will be developed in the future. Therefore, it will be necessary to evaluate more precisely the

roughness influence to hull frictional resistance based on experimental, theoretical, and numerical results.

The RC suggests the following items for the future:

(i) Continue to monitor trends and new developments in measurement techniques of hull roughness.

(ii) Continue to review trends in roughness definition considering estimation of roughness allowance.

(iii) Continue to monitor new developments in experimental techniques for roughness allowance estimation.

(iv) Continue to monitor new developments in theoretical and numerical estimation techniques for roughness influence to frictional resistance increase.

6. UNSTEADY FREE SURFACE

Experimental tow tank and full-scale measurement techniques have focused on unsteady flows and free-surface phenomena including wave breaking. These techniques have been motivated by interest in wave impact and slamming, spray generation, air entrainment/bubble generation, and wave breaking. The experimental work has focused on fundamental understanding as well as model development and code validation. Recent examples of full-scale field measurements include Beale et al, (2010), Drazen et al (2010), and Fu et al, (2012), and of laboratory-scale measurements by Masnadi et al (2013), Wang et al (2012), and Andre and Bardet (2014a and 2014b). While work in this area began in earnest back in 2004 with laboratory work utilizing laser induced fluorescence methods, free-surface flow visualization extends back to the 1990s, Dong et al (1998) and Waniewski (1998) for example (see Figure 31). These laser fluorescence methods were initially utilized to measure the free-surface of non-breaking flow fields (see Duncan, 1999), but were soon extended to breaking waves, see Kiger & Duncan (2012) and multiphase flows (Fu et al, 2009).

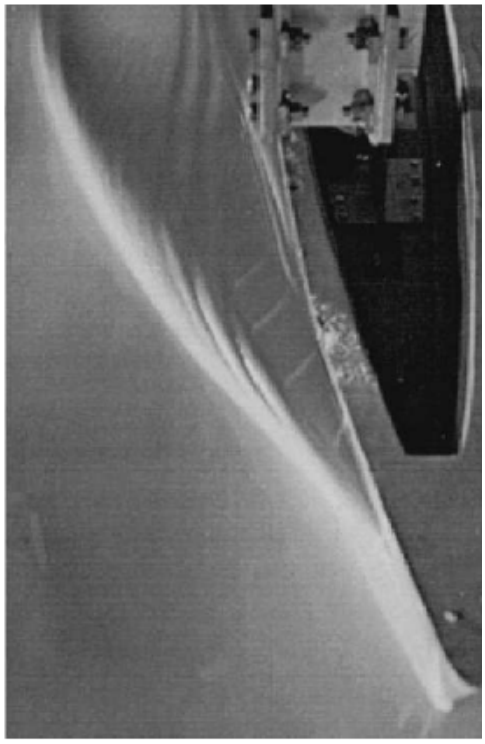

Figure 31. Sample image of the overhead view of the bow wave generated by towing a ship model, from Dong et al (1998).

While standard planar laser induced fluorescence (PLIF) has been used to identify 2-dimension wave profiles, only recently have they been extended to 3-dimensions and coupled with PIV measurements. Figure 32 (courtesy of Philippe Bardet) shows a conceptual test of multiple simultaneous PLIF planes recorded with a single camera.

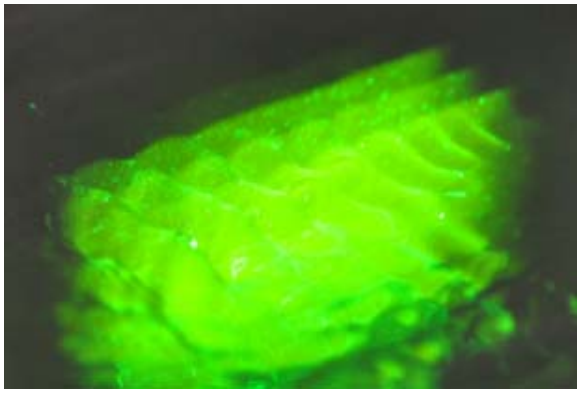

Figure 32. A Multi-plane PLIF sample to demonstrate principle of optical configuration for 3-D surface profile reconstruction (courtesy of Philippe Bardet).

The lower cost of high-resolution digital cameras and the development light field-imaging which involves sampling a large number of light rays from a scene to allow for scene reparameterization (Isaksen et al, 2000) and synthetic aperture refocusing, Synthetic aperture refocusing allows individual planes in the scene to be focused on, while planes not of interest are blurred and has allowed for the development 3-D imaging systems capable of simultaneously measuring a fluid volume and "seeing-through" partial occlusions (see Belden et al, 2010; Belden et al, 2011; and Belden and Techet, 2014).

While development of sophisticated 3-D techniques are being developed for simultaneous measurement of the free-surface and velocity field, work also continues on techniques to measure the unsteady free-surface in the field. Scanning LiDAR systems have been mounted on-board ships to document the unsteady free-surface and wave breaking (Terrill & Fu, 2008). More recently airborne LiDAR systems have been used to characterize the open ocean wave field and to validate radar based wave measurement systems. Similarly scanning LiDAR systems have been used in tow tank facilities (Fu et al, 2009), but their uncertainty and the need for surface roughness to provide sufficient backscatter limits their usefulness in scale model testing. Figures 33-37 show examples of the scanning LiDAR's capabilities.

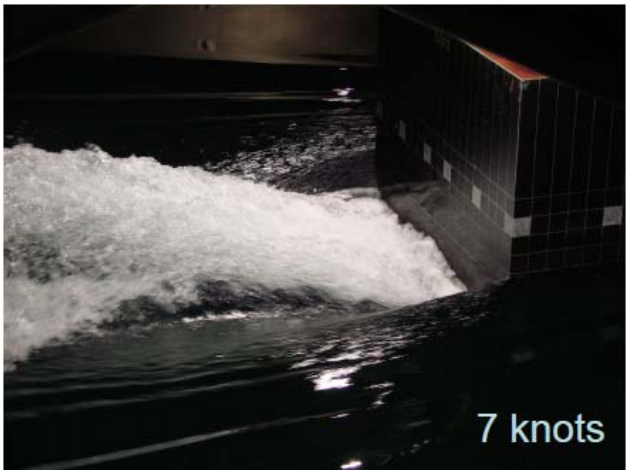

Figure 33. Image of the breaking transom wave generated by NSWCCD Model 5673 towed at 7 knots.

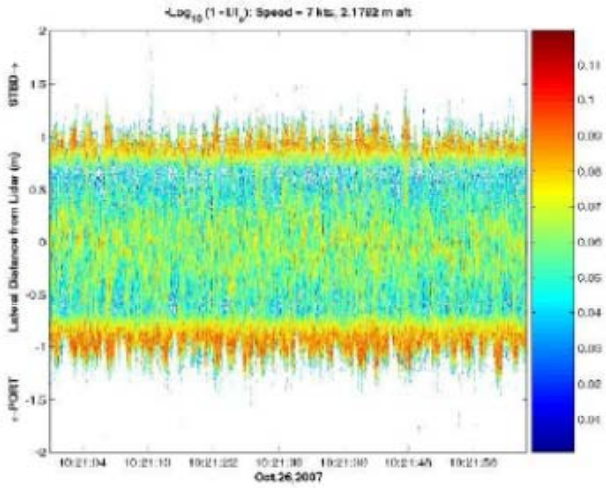

Figure 34. Pseudo-coloured time series of the LiDaR signal return amplitude 1.5 m (5 ft) aft of the transom. Model traveling at 7 knots.

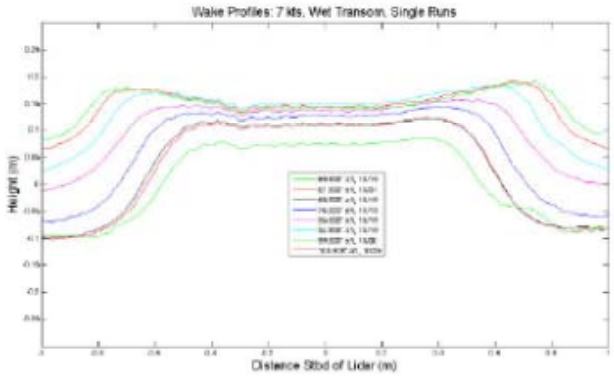

Figure 35. Mean transom wave elevation profiles of NSWCCD Model 5673 traveling at 7 knots.

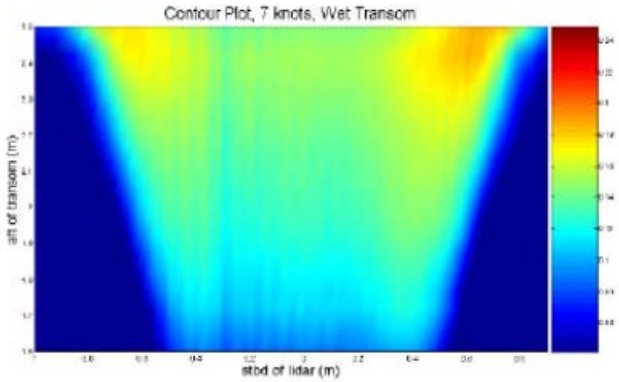

Figure 36. Contour plot of the mean free-surface elevation of the transom wave generated by NSWCCD Model 5673 at 7 knots.

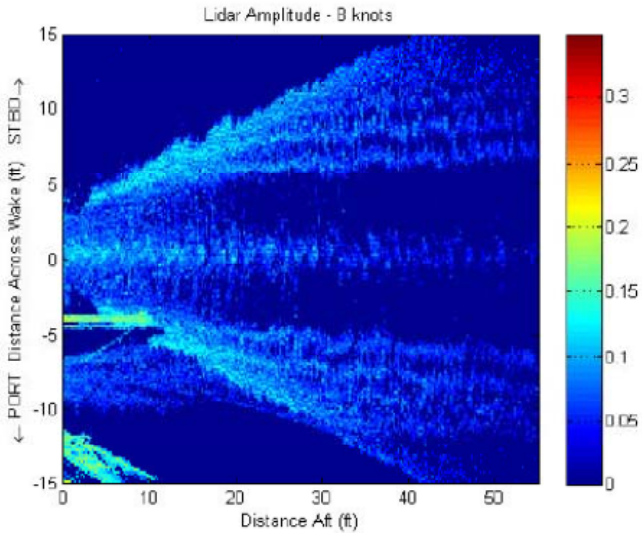

Figure 37. LiDAR image of the free-surface transom wave from NSWCCD Model 5673 traveling at 8 knots generated by panning the scanning the LiDAR aft at 3 deg/sec.

So the measurement and simulation of unsteady free surface flows remains and active area of research. Along with this work in developing measurement techniques and fundamental understanding is the long term need for better comprehension these mechanisms on added resistance. That is, our ability to use unsteady surface fluctuations and relate them back to resistance.

7. MODEL MANUFACTURE

The ability to change the geometry of a physical model has often required a significant extra expense which has restricted the ability to seek optimal hull form solutions at model scale. The development of new manufacturing techniques that can provide a cost-effective way forward for investigation of parametric changes to local hull features or appendage arrangement will allow more effective use of towing tank testing for problems where CFD still has limited applicability due to the need to resolve small computational time steps. The area of rapid manufacturing technology is actively

evolving and even during the duration of the 27th ITTC has both reduced in price and increased in capability. In the area of its application to ship models and the obvious area of ship model appendages there is a lack of published data on the accuracy with which models can be generated. Whereas it is evident that complex features, e. g. generation of turbulence trips can be built into the model or recesses for pressure sensors what needs more effort is in metrology of the finished products to assess the influence of the manufacturing technique on the actual accuracy and crucially the surface finish. For use in larger models there are often size limitations on the production of components and so models need to be made from many segments which need joining in a precise manner. Notwithstanding these limitations, it is expected that as material costs drop further many more components will be manufactured. A review by Vaezi et al (2013) considers the next generation devices which allow variable material properties and alternative materials to be generated in the same component.

7.1 Rapid Prototyping Technology

Rapid prototyping is an extremely important technology to both the commercial and military sectors. It is quickly becoming a mainstream technology for the production of models to evaluate fit and form or tooling for low volume manufacturing, see Freitag et al (2003) and Nguyen and Vai (2010) for a more complete summary of Rapid Prototyping.

The part to be built is first constructed as a solid model in a 3D modeling system and then exported through a file exchange format, typically the STL (Stereo Lithography) format. In an STL file, the surfaces of a model are represented by triangular polygons. Some rapid prototyping systems also accept IGES or DXF formats. A rapid prototyping machine reconstructs the model from the input file and slices it at relatively small increments, which may vary from 1/1000" (0.025mm) to 1/250" (0.1mm). Each layer is built and stacked on top of the previous layer, until the entire model is generated.

Rapid Prototyping Techniques. Stereo Lithography: With this method, each layer is generated by exposing the surface of a photosensitive liquid polymer, contained in a tank, to a laser beam that traces the section. The exposed area solidifies and is lowered by exactly the thickness of the layer. After all the layers have been generated the part is post-cured to harden the material. The size of the model is restricted by the size of the tank.

Laser Sintering. This process uses a laser beam to solidify particles of a powdered material. After a layer has been exposed, a new layer of powder is applied and exposed. The unexposed powder also functions as a support for extended and free floating parts of the model. This process may use a variety of powder materials, such as PVC, ABS, nylon, polyester, polypropylene, polyurethane, wax, or powdered metals.

Inkjet and 3D Printing. Unlike Laser Sintering, the laser is replaced with an inkjet head that deposits a liquid adhesive onto the powder as it translates across the surface. Key advantages of this process are the potential for increased productivity through the application of multiple inkjet heads and the ability to spatially introduce a second phase directly as part of the liquid adhesive.

Masking Process. With this method a black toner mask is generated on a glass plate which is the negative image of the layer to be built. A thin layer of liquid polymer is applied to the plate and is exposed to UV light. The un-

masked area solidifies when exposed and is attached to the previous layer.

Fused Deposition Modeling. With this method a thin plastic or wax like wire filament is fed to a moving head, which traces the area of the layer and deposits the filament on the surface. Just before deposition, the wire is heated above its solidifying temperature. Once deposited, the material solidifies and adheres to the previous layer.

Laminated Object Manufacturing. After a thin sheet of paper like material is positioned on a platform, a laser cuts the outline of the layer. The unwanted pieces of the layer are removed before the next sheet is placed on top. The layers are laminated together with a heat sensitive coating.

Cost of Rapid Prototyping. The price of a rapid prototyping machine currently ranges from $5,000 to $500,000. However, a number of service bureaus specialize in building rapid prototyping models and do it at a relatively low cost. 3D Printers are in general use and its cost depends on the time and material used. While the number of polygons that define a part is a minor factor, the volume and layer resolution of a part affect the production time as well as the quantity of material consumed and ultimately determine the cost. Small parts can be built relatively cheap but large parts cost is quite high.

Potential Use of Rapid Prototyping in Model Production. In general, paraffin wax, wood, foam and glass reinforced plastics are materials for manufacture of hull models. Wood is still probably the more commonly used. Rapid prototyping technology is quite expensive for model manufacturing purpose for today but appendages such as shaft, barrel, rudder and strut could be produced with extremely high precision. In addition, a shaft, barrel and bracket system could be manufactured perfectly in single stage using 3D printers as shown in Figure 38. Figure 39 shows installed system to model after painting phase.

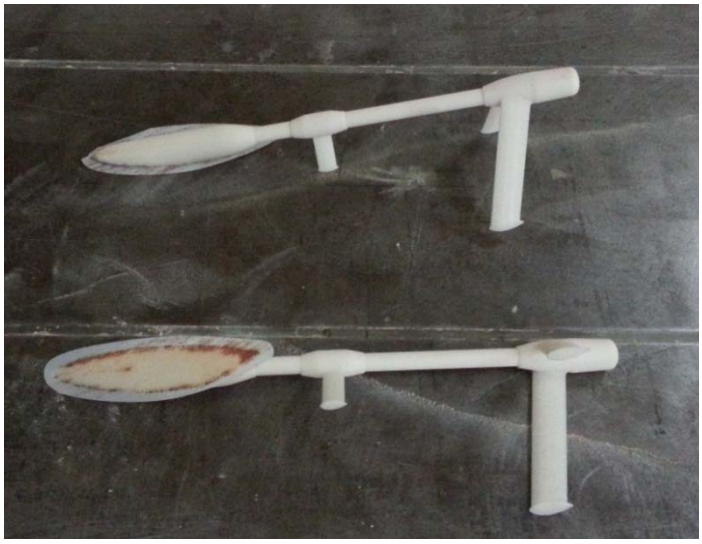

Figure 38. Shaft, barrel, strut and stern tube system (3D Printer used).

Figure 39. Installed shaft, barrel, strut and stern tube systems on a model in ITU Ata Nutku Ship Model Basin, Istanbul, Turkey.

7.2 Example of use of rapid prototyping technology in model testing

Limited publications have detailed the use of rapid prototyped components. A student project by Cope (2012) provide evidence of possible applications. Cope used a fused deposition technique and an ABS-M30 plastic to manufacture a 0.17m diameter propeller for a free running model. The printing process limited the minimum trailing edge thickness to 2 mm and required a modification to the scaled propeller thickness distribution. As ABS is not particularly stiff and has a degree of water permeability the propeller was copper-nickel plated with a thickness of 0.1 mm. An assessment was made of the increase of blade stiffness as shown in Table 13.

Table 13 Relative Stiffness of ABS Model Scale Propeller.

Blade Material	Relative Stiffness
ABS FDM	1
Cu+Ni Plated ABS	27
Aluminium Alloy	69

8. SIMULATION BASED DESIGN

The development in the computational power available and the relative maturity of the hydrodynamic analysis tools have significantly advanced simulation based design (SBD). The following section focuses on the different elements of SBD and the associated technological developments. These include developments related to global optimisation strategies, multi-objective optimisation, variable fidelity approaches, meta-models and geometry modelling. For various examples of the practical application of SBD the reader is referred to the cited literature and the references therein as well as the recent proceedings of the PRADS, FAST and IMDC conferences.

8.1 Optimization problem

The optimisation problem is commonly formulated as a nonlinear programming (NLP) problem (Tahara et al, 2011)

$$\min_{\bar{x}} \mathbf{f}(\mathbf{x},\mathbf{u}(\mathbf{x})),\ \mathbf{x}\in \mathrm{X}\subseteq \Re^{\mathrm{M}}$$
$$\begin{cases} h_j(\mathbf{x})=0,\ \ j=1,...,p \\ g_j(\mathbf{x})\le 0,\ \ j=1,...,q \\ x_i^l \le x_i \le x_i^u \end{cases} \qquad (17)$$

where **f** is a N-dimensional vector of objective functions, **x** is a vector of design variables belonging to a subset X of the M-dimensional real space, **u** is a vector of the state of the system, h_j and g_j are the equality and inequality constraints respectively, and the superscripts l and u refer to the lower and upper bounds of a specific design variable respectively.

Objectives. The optimisation algorithm tries to minimise or maximise the objective function or functions. Various objectives have been used in literature. The hydrodynamic objectives studied include wave making, total and added resistance, propulsion power, wake quality, wake wash and seakeeping merit functions. However, non-hydrodynamic objectives may also be of interest such as objectives related to structural performance, capacity, manufacturing or operating costs.

Depending on the number of objectives of interest the problem is either of single- or multi-objective type. Real-world design problems are associated with several, often conflicting, objectives. Thus, there is a growing interest in multi-objective optimisation (see e.g. Tahara et al, 2011; Kuhn et al, 2010). A multi-

objective problem can be a multi-disciplinary problem or a multi-point problem. In the former the objectives are related to different disciplines (e.g. resistance and seakeeping, Tahara et al, 2008, 2011), whereas in the latter the same objective function is evaluated at different condition (e.g. resistance at several speeds, Kandasamy et al, 2013). The multi-objective problem can be reduced into a single-objective problem through scalarisation, i.e. by forming a single objective as the weighted sum of the multiple objectives (see e.g. Tahara et al, 2011). For the weighting the knowledge of a designer, builder or owner can be used. However, often it is preferred that the Pareto optimality of the problem is maintained. For a Pareto optimal solution the improvement in one objective leads to a decline in one or more of the other objectives. Maintaining the Pareto optimality gives the designer a wider choice of optimal solutions and freedom to choose the weighting of the objectives afterwards.

The fundamental problem related to the objectives is that in ship hydrodynamics they are often expensive to evaluate. Furthermore, the problem has often multi-modal nature, i.e. the objective function has many local optima. These have a great influence on the choice of the optimisation strategy.

Design variables. The design variables dictate the possible changes to be explored in the optimisation process. The choice of correct design variables is fundamental for the quality of the optimal solution. The number of design variables, which determines the dimensions of the search space, should be as low as possible but still allow sufficient flexibility in the design variations. The hull fairness and limitations of manufacturing should also be considered when making the choice. The knowledge of a designer can be used to guide the selection of relevant variables, but also to reduce the dimensions of the search space. Sensitivity studies can also be used to support the choice of the variables and to determine dominating variations. Recently Proper Orthogonal Decomposition (POD) has been suggested for reduction of the dimensionality of the design space with the majority of the geometric variability retained. Chen et al (2014) have used POD in the optimisation of the water-jet propelled Delft Catamaran. They have managed to reduce the 20-dimensional design space into 4 and 6 dimensional spaces depending on the constraints and at the same time maintain 95 percent of the geometric variation.

The design variables are also subject to various constraints. The constraints can be in the form of equality or inequality constraints, they can be linear or nonlinear and they can constrain the design variables directly (e.g. box constraints) or indirectly (e.g. constraint on displacement). Because of the constraints the search space can be non-convex or even discontinuous. This limits the set of applicable optimisation algorithms. Furthermore, the way in which constraints are taken into account depends on the algorithm. This may be based on direct elimination of infeasible solutions, penalty formulation by increasing (or decreasing) the objective function, if constraints are violated or explicitly adjusting the search direction to point back into the feasible space.

Operating conditions. In the most common case in the literature the optimisation is performed for a single operating condition. However, a growing trend in the research is the optimisation for multiple operating conditions (multi-point optimisation). The variables defining the operating condition include for example ship speed, loading condition, water depth and sea state. These should be included in the statement of the optimisation problem. Operational profiles can be used to weight the different operating conditions.

Deterministic vs. stochastic problem. In the literature the optimisation problem is often considered as a deterministic problem. However, uncertainties in the real world operating (loading, trim, speed) or environmental conditions (sea state, wind, water quality) lead to a stochastic problem. In addition, there are various other sources of uncertainty such as the deviation between the intended and the manufactured design and modelling and numerical uncertainties in the evaluation of the objective functions. The practical consequence of this is that a design optimised for the expected values of the uncertain operating parameters may not be the real optimum of the stochastic problem.

Recently the stochastic nature of the real-life problems has gained more attention. Diez et al (2012) discuss the associated idea of robust design optimisation (RDO) extensively and present a RDO framework combining multi-disciplinary analysis and Bayesian decision making. Here the operating scenario is given as a probability distribution and the optimisation is based on the minimisation of the expectation of the objective function. They demonstrate RDO for the hydroelastic optimisation of the efficiency of a fin keel subject to uncertain yaw angle. Even if the design space is limited and the operating scenario is simple the stochastic and deterministic optima are different with the robust design showing a better overall performance.

8.2 Simulation based design framework

A SBD toolbox consists of three elements: (i) generation of a geometry based on the design variables, (ii) evaluation of the objective functions using the given geometry and (iii) optimisation algorithm which modifies the design variables based on the evaluated objectives. These steps are iterated until the optimum has been found or a set number of iterations has been reached.

Geometry modification. The geometry modification routine takes as input a set of design variables and produces as output a definition of geometry which can be a surface definition or a computational grid. The approaches for geometry modification can be categorised based on how their operation is related to the Computer Aided Design (CAD) systems:

- CAD free: works independently of any CAD system; might work directly on the computational grid
- CAD direct control: controls a real CAD system
- CAD emulation: emulates the operations that would normally be done in a CAD system; uses the same geometry entities and file formats to be compatible with a CAD system

Various algorithms have been proposed for the geometry modifications. In some algorithms the design variables are directly related to the points on the hull surface. In this case particular care has to be exercised in order to ensure hull fairness. For example, the hull can be modified by multiplying the hull offsets with smooth functions (Tahara et al, 2011; Zhang and Ma, 2011) or by interpolating the displacements using radial basis functions (Kim et al, 2010), where the parameters of the functions are defined by the displacement of a set of hull surface points.

Alternative approaches have been proposed, where the design variables are independent of the hull surface definition. Two methods showing good performance and great flexibility are the geometry morphing (see e.g. Kang and Lee, 2012) and the free form deformation (FFD, see e.g. Tahara et al, 2011). In morphing two or more hull forms are combined into one as a

weighted sum of the parent forms. The number of weights is usually one less than the number of parent hull forms. By using the weights directly as design variables, an optimisation algorithm with very low number of design variables is achieved. In FFD, on the other hand, the hull or a part of it is enclosed in a parallelepiped containing a structured set of control points. The parallelepiped is deformed by moving the control points, and the displacement of any point inside it is interpolated based on the displacements of the control points (for details see e.g. Tahara et al, 2008). Several parallelepipeds can be combined to perform global and local modifications of the hull form.

Global modification approaches operating on the parameterisation of the common ship design curves (e.g. sectional area curve, waterline, profile, sections) have also been proposed (see e.g. Kim et al, 2008). Dedicated, fully analytical approaches have been presented for particular hull forms (e.g. rounded bilge boats by Pérez and Clemente, 2011). The benefit of these methods is that there is a direct link to the classical design office practice, and the modifications are easily related to the changes in the established design parameters. Based on the parameterisation it is also possible to formulate a constrained design approach, in which the geometry will automatically satisfy the constraints set on the main parameters such as buoyancy, longitudinal centre of buoyancy or waterline area (Pérez and Clemente, 2011).

Analysis tools. The analysis tools take as inputs the modified geometry and the operating conditions and produce values of the objective functions and possible constraints. The level of detail of the methods used varies a lot. The tool set is a compromise affected by for example the complexity of the design problem (number of design variables and objective functions, multidisciplinary problems), the time and computational resources available and the requirements on the accuracy. In concept level design the problem is multidisciplinary, the search space is large and the time to find the optimum is very limited. Here simulation is too time consuming and the tools may be very simple based on design equations, regression data or correlation lines (see e.g. Hart and Vlahopoulos, 2010). When simulations can be afforded, potential flow based tools provide more accuracy, but are still relatively efficient. The full range of potential flow based methods ranging from thin ship theory to fully nonlinear boundary element methods have been used in SBD (Kim et al, 2010; Zhang and Ma, 2011; Tahara et al, 2011). The most accurate, but also computationally most expensive methods used so far in SBD are mainly based on the Reynolds-Averaged Navier-Stokes (RANS) equations (see e.g. Kim et al, 2008; Tahara et al, 2008, 2011).

Optimisation algorithms. The optimisation algorithm of the SBD framework works on the values of the objective functions produced by the analysis tools and tries to find a better set of design variables leading to an improved value of the objective or objectives. In gradient based algorithms the optimisation is driven by the gradient of the objective function, whereas gradient free algorithms operate without any knowledge of the gradient. The optimisation algorithms can also be categorised into local and global algorithms based on whether they search for local or global optima. The literature cited in this chapter includes various examples of optimisation algorithms that have been used in SBD and comparisons of common algorithms (see e.g. Kim et al, 2008; Campana et al, 2009).

The trend has been towards gradient free global optimisation algorithms. There are several reasons for this. (i) The gradient evaluation is problematic due to noisy and non-smooth objective functions or due to unavailability of

derivatives, so that local algorithms could be stuck at local minima. (ii) The geometrical and functional constraints required to make the design realistic result often into nonconvex feasible search space. (iii) In several fields experimental and computational activities have helped the designers to produce near optimal designs, so that finding further improvement with local optimisation is difficult. (Campana et al, 2009) However, local algorithms complement global algorithms with different advantages such as faster convergence. Therefore, hybrid algorithms combining global and local algorithms have also been proposed. (see e.g. Campana et al, 2009; Peri and Diez, 2013)

The rapid development of parallel computing has led to the increasing popularity of population based optimisation algorithms. Many of these draw their inspiration from the processes in nature. These include various forms of evolutionary algorithms (EA), such as evolution strategies (ES) and genetic algorithms (GA; Tahara et al, 2008; Kim et al, 2010; Zhang and Ma, 2011; Kandasamy et al, 2013), and particle swarm optimisation (PSO; Kim et al, 2008; Campana et al, 2009; Hart and Vlahopoulos, 2010; Diez et al, 2012; Tahara et al, 2011; Kandasamy et al, 2013). In EAs the main idea is to produce successive generations of designs which exhibit improving performance. The main operations between generations are selection, recombination (crossover) and mutation. The differences between the various EA methods lie in the details of these operations and how the operations are combined. In PSO the global optimum is sought for based on an analogy with the behaviour of a flock of birds. Each individual of the swarm explores the search space with a variable velocity. This is affected by the previous velocity (inertia), by the attraction of the best locations so far for the swarm (social factor) and for the individual (cognitive factor). The original PSO formulation has additionally randomness included, but deterministic variants have also been successful applied (Campana et al, 2009).

Regardless of the type of the algorithm, in multi-modal problems it is essential that there is a balance between the local and exploring characteristics of the algorithm. A good balance leads to a fast convergence of the algorithm and avoids premature convergence to a local optimum. The balance can be changed as the solution approaches the global optimum. For example, in PSO the inertia controls the balance between the local and global characteristic. (Campana et al, 2009)

The computational expense of the evaluation is often a problem in optimisation. The computational cost can be reduced by using meta-models, variable fidelity/physics approach or a combination of these. The idea here is that the number of the most accurate and expensive evaluations is reduced by performing the majority of the evaluations with less expensive approach. For example, the expensive method is called only, if the less accurate method shows an improvement in the design. A meta-model is an approximation for the behaviour of the objective function constructed from the function values at a set of sample points. In variable physics approach the low fidelity solution could be based on low cost potential flow solution and the high fidelity solution on a RANS solver (see e.g. Tahara et al, 2008, 2011; Kandasamy et al, 2013). Alternatively a variable resolution or iterative accuracy approach could be used. In the former the low and high fidelity solutions are obtained with a coarse and a fine discretisation resolution, respectively. In the latter, the convergence level of the numerical solution is altered between the fidelities. Meta-models based on the known difference between the high and low fidelity solutions at sample design points can be used to improve the low fidelity estimate, and a trust region

methodology can be used to control the frequency of high fidelity evaluations.

The effectiveness of the variable physics approach was demonstrated by Kandasamy et al (2013). They combined a low-fidelity potential flow code and a high-fidelity RANS code for the resistance optimisation of the water-jet propelled Delft Catamaran. With the variable-fidelity approach the overall CPU time dropped to less than half of the high-fidelity approach, and both approaches converged to the same optimum. A further, and more significant, reduction in computational effort for the same optimisation problem is achieved by Chen et al (2014). They studied the combination of POD for the dimensional reduction of the design space, multiple meta-models and multiple deterministic PSO variants. The deterministic PSO gave the same optimum as the original stochastic version of PSO, but with just 2% of the computational cost. Compared to Kandasamy et al (2013) the proposed approach provided an additional calm-water resistance reduction of 6.6% with 1/10th of the computational cost.

Verification and Validation. In order to have confidence in a SBD framework the results of the optimisation process should be verified and validated (V&V), i.e. a simulated improvement should correspond to a real-life improvement with a sufficient confidence. It has been proposed that the methodology used for the V&V of single run cases can be extended into a systematic procedure for the V&V of the optimised solution. This V&V process consists of three parts and is based on the difference in performance between a parent and optimised designs. (i) The optimised design is numerically verified, if it can be shown that the magnitude of simulated improvement is larger than the numerical uncertainty. (ii) The optimised design is experimentally verified, if the magnitude of the measured improvement is larger than the experimental uncertainty. (iii) The optimised solution is validated, if the absolute value of the difference between the simulated and measured improvements is less than the combined uncertainty from the simulations and the measurements (Tahara et al, 2008, 2011).

It should be noted that the methodology is independent of the V&V of the individual solutions for the parent and optimal design and only includes the trend. This is in line with the fundamental goal of the design problem, i.e. to find the optimal design. The absolute values of individual designs can be verified and validated using a single run procedure.

For practical examples of the application of the V&V methodology the interested reader is referred to Tahara et al (2008, 2011) and Kandasamy et al (2013).

9. RECOMMENDATIONS

The 27th ITTC Resistance Committee recommends the following:

- Adopt the updated guideline 7.5-02-02-02 Testing and Extrapolation Methods, General Guidelines for Uncertainty Analysis in Resistance Towing Tank Tests

- Adopt the updated guideline 7.5-02-02-02.1 Testing and Extrapolation Methods, Example Uncertainty Analysis of Resistance Tests in Towing Tank which effectively replaces the dropped 7.5-02-02-02(2002, rev.01).

- Adopt the new guideline 7.5-02-02-02.2 Testing and Extrapolation Methods, Practical Guide: Uncertainty Analysis of Resistance Measurement in Routine Tests.

- Remove the procedure 7.5-02-02-03 Testing and Extrapolation Methods, Resistance, Uncertainty Analysis Spreadsheet for Resistance Measurements.

- Remove the procedure 7.5-02-02-04 Testing and Extrapolation Methods Resistance, Uncertainty Analysis Spreadsheet for Speed Measurements.

- Remove the procedure 7.5-02-02-05 Testing and Extrapolation Methods Resistance, Uncertainty Analysis Spreadsheet for Sinkage and Trim Measurements.

- Remove the procedure 7.5-02-02-06 Resistance uncertainty analysis spreadsheet for wave profile measurements.

10. CONCLUSIONS

It is the need to increase energy efficiency of shipping that drives the need to significantly improve our ability to measure resistance.

10.1 State of the Art

The state-of-the-art review captures the most significant developments. There is an increased need to do higher precision resistance measurements and understand trade-off between resistance components. Trim optimisation requires enhanced precision in resistance test e.g. 1%, improvements need to be able to resolve to greater than this accuracy. There is the capability to acquire more data during test motion e.g. wireless sensors, synchronised video, better documentation for CFD validation, and improve standard of reporting of test conditions. There is some new limited validation data, and preparation for the Tokyo 2015 CFD workshop will give validation for a new ship type. It is noted that there is still a lack of high quality data for high performance craft e.g. planning/hydrofoil craft.

The increasing availability of computational resources means that mesh resolution is less of an issue, however noting the recent 32 billion cell alters perspective but need to get better handle on 'real' cost of such analysis. Many challenges remain with breaking, bubbly flow, and spray will have an impact for resistance. It may not change the value but alters detail of flow which may have implications for propulsion etc. This links into need for new R&D – surface roughness, model construction/precision, aim to reduce uncertainty and better understanding.

With regard to procedures/guidelines, it was decided to eliminate the spreadsheet as they are were based on the AIAA standard and furthermore, not now relevant as they were primarily linked to the world wide campaign. The update to ISO GUM was applied as it is fairly straightforward and should be widely adopted in routine commercial tests. It should be noted that there is still no procedure for recording wave profile. The surface roughness guideline was not changed, but reviewed in the committee report for better understanding.

The worldwide campaign data should be made available via the new ITTC website. The previous committee has provided an easily used database for additional studies. Further analysis was conducted by the committee and has shown some greater understanding. No new data was received. We suggest an approach for inter tank bias comparison, established a base line by removing 'outliers' and make accessible the whole database via new ITTC website and will provide a searchable spreadsheet for use when looking at all data. A comparison is made with the corresponding data from the CFD analysis from Gothenburg 2010.

For future such campaigns, the double blind, although a good idea but in actuality, was too much of challenge, with limited participation and may have bias issues with 'changes' to the model during the campaign due to the extreme time scale of the effort.

With respect to surface roughness, limitations from practical systems available and challenge of getting measurements on full scale ships with vast area and looking at fine scale points resolved to height changes of a few mm. Need for new instrumentation systems perhaps.

Measurement of the unsteady free surface is still very much needed to support the development of breaking models and the validation of CFD codes. As the measurement techniques capable of characterising the small scale roughness associated with wave breaking are still very much in development, there is no need for a procedure at this time.

Model based manufacturing has definitely been impacted by the proliferation of rapid prototyping. The questions of whether large high fidelity physical models can be built from multiple pieces and how strength/stiffness are maintained remain to be answered.

Simulation based design has evolved rapidly in the past decade. A main driver of the development is the inherent computational cost of the simulations. There is an apparent trend towards hybrid algorithms, which combine analysis methods of varying fidelity. In these methods, the majority of objective function evaluations is performed with low-cost methods (potential flow, surrogate models) and the accuracy of the optimisation is guaranteed with infrequent high-cost evaluations (e.g. RANS). A careful setup of the design problem is required in order to keep the dimensions of the design space to a minimum. At the same time the geometry manipulation methods should be able to guarantee a smooth geometry. Geometry morphing and free form deformation have proven to be favoured choices in this respect. Recently, significant reduction in the computational cost has been obtained by using proper orthogonal decomposition to reduce the number of design variables and at the same time keeping nearly all of the geometric variability. As the approaches for deterministic problems start to mature, it is expected that the stochastic nature of the design problems (e.g. variable environment in terms of seastate/wind, operational profile) will gain more attention.

10.2 Potential Tasks for the 28th ITTC Resistance Committee

(i) Develop a new procedure for wave profile measurement and wave resistance analysis, uncertainty analysis for extrapolation can then engage possible alternative scaling techniques in a rational way

(ii) Unsteady free surface dynamics is still an active area for research – and there remains a long term need for better comprehension of added resistance, that is the ability to use surface fluctuations and turbulence and relate them to resistance.

(iii) Resolve differences between ISO 4287 and widely used BMT roughness measurement system.

(iv) Propose an approach for tanks to reduce/manage their uncertainty as a follow on from the Worldwide Campaign.

(v) Sensitivity study for which areas of the ship should you be measuring/modifying roughness

11. REFERENCES

Andre, M.A. and Bardet, P.M., 2014a, "High Resolution Simultaneous Multiphase Time-Resolved Particle Image Velocimetry", 17th Int. Symposium on Applications of Laser Techniques to Fluid Mechanics.

Andre, M.A. and Bardet, P.M., 2014b, "Velocity Field, Surface Profile and Curvature Resolution of Steep and Short Free Surface Waves", Experiments in Fluids, in press.

Atlar,M and Wilczynski, L(eds), 2013, Proc. of 3rd Advanced Model Measurement Technology Conference , Gdansk,Poland

Avci, Atakan and Karagoz, Irfan, 2009, "A Novel Explicit Equation for Friction Factor in Smooth and Rough Pipes", Journal of Fluids Engineering, Vol. 22.

Beale, K.C., Fu, T.C., Fullerton, A.M., Drazen, D. and Wyatt, D., 2010, "An Experimental Characterization of Full-Scale Ship Generated Bow Spray," Proceedings of the 28th Symposium on Naval Hydrodynamics, Pasadena, USA.

Belden, J. and Techet, A.H., 2014, "Simultaneous Quantitative Flow Measurement using PIV on Both Sides of the Air-Water Interface for Breaking Waves", Experiments in Fluids, under review.

Belden, J., Truscott, T.T., Axiak, M., and Techet, A.H., 2010, "Three-dimensional Synthetic Aperture Particle Imaging Velocimetry," Measurement Science and Technology, 21(12), 2010.

Belden, J., Truscott, T.T., Ravela, S., Techet, A.H., 2011, "Three-Dimensional Synthetic Aperture Imaging and Resolution of Multi-Phase Flows", Proceedings of the ASME-JSME-KSME Joint Fluids Engineering Conference, Hamamatsu, Japan; 24-29 July.

Campana, E.F., Liuzzi, G., Lucidi, S., Peri, D., Piccialli, V., and Pinto, A., 2009, "New Global Optimization Methods for Ship Design Problems", Optimization and Engineering, Vol. 10, pp. 533-555.

Chen, X., Diez, M., Kandasamy, M., Zhang, Z., Campana, E.F., and Stern, F., 2014, "High-Fidelity Global Optimization of Shape Design by Dimensionality Reduction, Meta-Models and Deterministic Particle Swarm", Engineering Optimization, DOI: 10.1080 /0305215X.2014.895340.

Cope, D., 2012, "Design of a Free-running, 1/30th Froude Scaled Model Destroyer for In-situ Hydrodynamic Flow Visualization", SM Thesis, MIT

Diez, M., Peri, D., Fasano, G., and Campana, E.F., 2012, "Hydroelastic Optimization of a Keel Fin of a Sailing Boat: a Multidisciplinary Robust Formulation for Ship Design", Structural and Multidisciplinary Optimization, Vol. 46, pp 613-625.

Dong, R., Katz, J., and Huang, T.T., 1997, "On the Structure of Bow Waves on a Ship Model", Journal of Fluid Mechanics. 346. 77-115.

Drazen, D., Beale, K.L.C., Bhushan, S., Fullerton, A.M., O'Shea, T., Brucker, K., Dommermuth, D., Wyatt, D., Carrica, P., Fu, T.C., Stern, F., 2010, "Comparisons of Model-Scale Experimental Measurements and Computational Predictions for the Transom Wave of a Large-Scale Transom Model," Proceedings of the 28th Symposium on Naval Hydrodynamics, Pasadena, USA.

Eça, L. and Hoekstra, M., 2010, "Quantifying Roughness Effects by Ship Viscous Flow Calculations", Proceedings of the 28th Symposium on Naval Hydrodynamics, Pasadena, USA.

Eça, L. and Hoekstra, M., 2014, "A Procedure for the Estimation of the Numerical Uncertainty of CFD Calculations Based on Grid Refinement Studies", Journal of Computational Physics, Vol. 262, pp 104–130.

Freitag, D., Wohlers, T., and Philippi, T., 2003, "Rapid Prototyping: State of the Art," Manufacturing Technology Information Analysis Center.

Fu, T.C., Fullerton, A.M. and Drazen, D., 2009, "Free-Surface Measurements in a Tow Tank Using LIDAR," ASME 2009 Fluids Engineering Summer Meeting (FEDSM2009), Forum on Fluid Measurements and Instrumentation, Paper No. FEDSM2009-78464, Vail, Colorado, USA, August 2-6.

Fu, T.C., Fullerton, A.M., Ratcliffe, T., Minnick, L., Walker, D., Pence, M.L., and Anderson, K., 2009, "A Detailed Study of Transom Breaking Waves," Naval Surface Warfare Center Carderock Division, Hydromechanics Directorate R&D Report, NSWCCD-50-TR-2009/025, May.

Fu, T.C., O'Shea, T.T., Judge, C.Q., Dommermuth, D., Brucker, K., and Wyatt, D.C., 2013, "A Detailed Assessment of Numerical Flow Analysis (NFA) to Predict the Hydrodynamics of a Deep-V Planing Hull", International Shipbuilding Progress, Vol. 60, pp 143-169.

Geerts, S.,Van Kerkove, G, Vantorre, M, and Delefortrie, G, 2011, "Waterline registration using fluorescent lighting", Advanced Model Measurement Technology for EU Maritime Industry - AMT'11, Newcastle-upon-Tyne.

Guo, B.J., Deng, G.B., and Steen, S., 2013, "Verification and Validation of Numerical Calculation of Ship Resistance and Flow Field of a Large Tanker", Ships and Offshore Structures, Vol. 8, pp 3-14.

Hart, C.G., and Vlahopoulos, N., 2010, "An Integrated Multidisciplinary Particle Swarm Optimization Approach to Conceptual Ship Design", Structural and Multidisciplinary Optimization, Vol. 41, pp 481–494.

Hino, T., 2012, "Surface Roughness Models for CFD Simulations", Conference Proceedings of the Japan Society of Naval Architects and Ocean Engineers, Vol.15.

Huang, F., Yang, C., and Noblesse, F., 2013, "Numerical Implementation and Validation of the Neumann–Michell Theory of Ship Waves", European Journal of Mechanics - B/Fluids, Vol. 42, pp 47–68.

ISO, 1997, "Geometrical Product Specifications (GPS) - Surface Texture: Profile method - Terms, Definitions and Surface Texture Parameters", ISO 4287:1997.

ITTC, 1987, "Report of the Advisory Council", Proceedings of the 18th ITTC Full Conference, Kobe, Japan.

ITTC, 1990, "Report of the Panel on Validation Procedures", Proceedings of the 18th ITTC Full Conference, Madrid, Spain.

ITTC, 2005, "Final Report and Recommendations to the 24th ITTC by the Resistance Committee", Proceedings of the 24th ITTC Full Conference, 4-10 September, Edinburgh, UK.

ITTC, 2011a, "Report of Specialist Committee on Surface Treatment", Proceedings of the 26th International Towing Tank Conference, Rio de Janeiro, Brazil

.

ITTC, 2011b, "Report of Resistance Committee", Proceedings of the 26th International Towing Tank Conference, Rio de Janeiro, Brazil.

Isaksen, A., McMillan, L., and Gortler. S.J., "Dynamically Reparameterized Light Field", in SIGGRAPH'00: Proceedings of the 27th Annual Conference on Computer Graphics and Interactive Techniques, Number 1-58113-208-5, New York, NY, USA, 2000. ACM Press/Addison-Wesley Publishing Co., pp 297–306.

Kandasamy, M., Peri, D., Tahara, Y., Wilson, W., Miozzi, M., Georgiev, S., Milanov, E., Campana, E.F., and Stern, F., 2013, "Simulation Based Design Optimisation of Waterjet Propelled Delft Catamaran", International Shipbuilding Progress, Vol. 60, pp 277-308.

Kang, J-Y., and Lee, B-S., 2012, "Application of Morphing Technique with Mesh-Merging in Rapid Hull Form Generation," International Journal of Naval Architecture and Ocean Engineering, Vol. 4, pp 228-240.

Katsui, T., Izumi, T., and Ueno, S., 2011, "The Effects of Surface Roughness on Flat-Plate Frictional Resistance", Conference Proceedings of the Japan Society of Naval Architects and Ocean Engineers, Vol.13.

Kawakita, C., 2013, "Study on Marine Propeller Running in Bubbly Flow", Proceedings of the 3rd International Symposium on Marine Propulsors, Launceston, Tasmania, Australia.

Kawashima, H., Kodama, Y., Hinatsu, M., Hori, T., Makino, M., Ohnawa, M., Takeshi, H., Sakoda, M., Kawashima, H., and Matsuno, F., 2007, "A Research Project on Application of Air Bubble Injection to a Full Scale Ship for Drag Reduction", Proceedings of FEDSM2007 (5th Joint ASME/JSME Fluids Engineering Conference), San Diego, California USA.

Kawashima, H., Makino, M., Fukasawa, R., Takeshi, H., Kawaguchi, Y., Tuji, Y., Iwamoto, K., Motozawa, M., and Masuda, H., Mieno, H., 2012, "Effect of Geometric Roughness Parameters on Turbulent Frictional Resistance", Conference Proceedings of the Japan Society of Naval Architects and Ocean Engineers, Vol.15.

Kiger, K.T., Duncan, J.H., 2012, "Air-Entrainment Mechanisms in Plunging Jets and Breaking Waves", Annual Review of Fluid Mechanics, Vol. 44, pp. 563-596.

Kim, H., Yang, C., Kim, H., and Chun, H.H., 2010, "A Combined Local and Global Hull Form Modification Approach for Hydrodynamic Optimisation", Proceedings of the 28th Symposium on Naval Hydrodynamics, Vol. 2, pp 1219-1232.

Kim, H.J., Chun, H.H., Peri, D., and Campana, E.F., 2008, "Optimizing using Parametric Modification Functions and Global Optimization Methods," Proceedings of the 27th Symposium on Naval Hydrodynamics, Vol. 2, pp 1457-1468.

Kuhn, J., Collette, M., Lin, W.-M., Schlageter, E., Whipple, D., and Wyatt, D., 2010, "Investigation of Competition between Objectives in Multiobjective Optimization", Proceedings of the 28th Symposium on Naval Hydrodynamics, Vol. 2, pp 1233-1244.

Larsen, N.L., Simmonsen, C.L, Neilsen, C.K., and Holm, C.R., 2012, "Understanding the physics of trim". Ninth Annual Green Ship Technology Conference, Copenhagen, March 2012.

Larsson, L., Stern, F., Visonneau, M. (Eds.), 2014, Numerical Ship Hydrodynamics: An Assessment of the Gothenburg 2010 Workshop, Springer Science+Business Media, Dordrecht.

Larsson, L., Visonneau, M., Stern, F., Hino, T., Hirata, N., Kim, J., 2014, Communication with the Steering Committee of the CFD Workshop 2015.

Maki, K.J., Broglia, R., Doctors, L.J., Di Mascio, A., 2013, "Numerical Investigation of the Components of Calm-Water Resistance of a Surface-Effect Ship", Ocean Engineering, Vol. 72, pp 375- 385.

Masnadi, N., Washuta, N., Wang, A., and Duncan, J.H., 2013, "The Interaction of a Turbulent Ship-Hull Boundary Layer and a Free Surface", presented at the 66th Annual Meeting of the American Physical Society, Division of Fluid Dynamics, November 24-26, Pittsburgh, Pennsylvania, USA http://meetings.aps.org/link/BAPS.2013.DFD.D28.2.

Mieno, H., 2012, "An Experimental Study for Friction Resistance of Ship Hull Sprayed with Paints", Conference Proceedings of the Japan Society of Naval Architects and Ocean Engineers, Vol.14, Japan.

Molland, A.F., Turnock, S.R. and Hudson, D.A., 2011, Ship Resistance and Propulsion: Practical Estimation of Ship Propulsive Power, Cambridge University Press.

Molland, A.F., Turnock, S.R., Hudson, D.A., and Utama I.K.A.P, 2014, "Reducing ship emissions: a review of potential practical improvements in the propulsive efficiency of future ships." Transactions of Royal Institution of Naval Architects Part A, 156, 175-188.

Nguyen, Huy and Vai, Michael, 2010, "Rapid Prototyping Technology", Vol. 18, No 2, Lincoln Laboratory Journal.

Nishikawa, T., Yamade, Y., Sakuma, M., Kato, C., 2012, "Application of Fully-Resolved Large Eddy Simulation to KVLCC2 – Bare Hull Double Model at Model Ship Reynolds Number", Journal of the Japan Society of Naval Architects and Ocean Engineers, Vol. 16, pp 1-9.

Nishikawa, T., Yamade, Y., Sakuma, M., Kato, C., 2013, "Fully Resolved Large Eddy Simulation as an Alternative to Towing Tank Resistance Tests – 32 Billion Cells Computation on K computer", Proceedings of the 16th Numerical Towing Tank Symposium, Mülheim, Germany.

Olivieri, A., Pistani,F., Avanzini,A., Stern, F. and Penna, R., 2001, "Towing Tank Experiments of Resistance, Sinkage and Trim, Boundary Layer, Wake, and Free Surface Flow Around a Naval Combatant INSEAN 2340 Model", IIHR Technical Report No. 421, September, Iowa City, Iowa, USA

Pérez, F. and Clemente, J.A., 2011, "Constrained Design of Simple Ship Hulls with Image-Spline Surfaces", Computer Aided Design, Vol. 43, pp 1829–1840.

Peri, D. and Diez, M., 2013, "Ship Optimization by Globally Convergent Modification of PSO by a Surrogate-Based Newton Method", Engineering Computations, Vol. 30, pp 548-561.

Rodenhuis, G.S., Morgan, W.B. and Davies, M.E.H., 1987, "Validation and Uncertainty Analysis – An ITTC Activity Session 1: Report of Advisory Council Working Group on Validation", Proceedings of the 18th ITTC Full Conference, Kobe, Japan.

Sasajima, H., et.al. 1965, "Experimental Investigation into Roughness of Hull Surface and Increase of Skin Frictional Resistance", J. of Zosen Kiokai, Vol. 117, pp 58-71.

SIMMAN 2014, DTMB 5415 Geometry and Conditions, http://www.simman2014.dk/.

Stern, F., Longo, J., Penna, R., Olivieri, A., Ratcliffe, T. and Coleman, H., 2000, "International Collaboration on Benchmark CFD Validation Data for Surface Combatant DTMB Model 5415", 23rd ONR Symposium on Naval Hydrodynamics, Val de Reuil, France.

Stern, F., Yang, J., Wang, Z., Sadat-Hosseini, H., Mousaviraad, M., Bhushan, S., Xing, T., 2013, "Computational Ship Hydrodynamics: Nowadays and Way Forward", International Shipbuilding Progress, Vol. 60, pp 3-105.

Tahara, Y., Peri, D., Campana, E.F., and Stern, F., 2011, "Single- and Multi-objective Design Optimization of a Fast Multihull Ship: Numerical and Experimental Results", Journal of Marine Science and Technology, Vol. 16, pp 412–433.

Tahara, Y., Peri, D., Campana, E.F., and Stern, F., 2008, "Computational Fluid Dynamics-Based Multiobjective Qptimization of a Surface Combatant Using a Global Optimization Method", Journal of Marine Science and Technology, Vol. 13, pp 95–116.

Takai, T., Kandasamy, M., Stern, F., 2011, "Verification and Validation Study of URANS Simulations for an Axial Waterjet Propelled Large High-Speed Ship", Journal of Marine Science and Technology, Vol. 16, pp 434-447.

Takinaci, A.C., Onen, M., 2013, "Low Engine Power-Less Emission", Atmos 2013, 6th Atmospheric Science Symposium, İstanbul Turkey, pp 193-200.

Tanaka, H., Toda, Y., Higo, K., and Yamashita, K., 2003, "Influence of Surface Properties of Coatings to Frictional Resistance", Journal of the Kansai Society of Naval Architects, Vol. 239, Japan.

Taravella, B.M., and Vorus, W.S., 2012, "A Wave Resistance Formulation for Slender Bodies at Moderate to High Speeds", Journal of Ship Research, Vol. 56, pp 207-214.

Terrill, E.J., and Fu, T.C., 2008, "At-Sea Measurements for Ship Hydromechanics", Proceedings of the 27th Symposium on Naval Hydrodynamics, Seoul, Korea, October 5-10.

Vaezi, M, Chianrabutra, S, Mellor, B and Yang, S., 2013, "Multiple material additive manufacturing – Part 1: a review". Virtual and Physical Prototyping, 8, (1), 19-50

Wang, D., Dai, D., Liu, X., and Duncan, J.H., 2012, "An Experimental Study of Droplets Produced by Plunging Breakers", presented at the 65th Annual Meeting of the American Physical Society, Division of Fluid Dynamics, Nov. 18-20, San Diego, CA, USA, http://meetings.aps.org/link/BAPS.2012.DFD.D28.3.

Waniewski, T.A. 1998. "Air Entrainment by Bow Waves", Ph.D. thesis, California Institute of Technology, October.

Weinell, C.E., Olsen, K.N., and Christoffersen M.W., 2003, "Experimental Study of Drag Resistance Using a Laboratory Scale Rotary Set-Up", Biofouling, International Congress on Marine Corrosion and Fouling, No.11, San Diego, California, USA.

White, F.M., 1991, "Viscous Fluid Flow," 2nd Edition, McGrawHill.

Winden, B., Turnock, S.R., and Hudson, D.A., 2013, "Predicting powering performance changes for ships in offshore conditions from small design modifications," Twenty-Third International Offshore and Polar Engineering Conference, Anchorage, Alaska, USA.

Winkel, E.S., Cutbirth, J.M., Ceccio, S.L., Perlin, M., and Dowling, D.R. 2012, "Turbulence Profiles from a Smooth Flat-Plate Turbulent Boundary Layer at High Reynolds Number," Experimental Thermal and Fluid Science, Vol. 40, pp 140–149.

Yan, H., Liu, Y., 2011, "An Efficient High-Order Boundary Element Method for Nonlinear Wave-Wave and Wave-Body Interactions", Journal of Computational Physics, Vol. 230, pp 402-424.

Zhang, B.-J. and Ma, K., 2011, "Study on Hull Form Optimization for Minimum Resistance Based on Niche Genetic Algorithms", Journal of Ship Production and Design, Vol. 27, pp 162-168.

Zou, L and Larsson, L, 2014, "A verification and validation study based on resistance submissions", Numerical Ship Hydrodynamics: An Assessment of the Gothenburg 2010 Workshop, Springer Science+Business Media, Dordrecht.